

GT23D-Bench: A Comprehensive General Text-to-3D Generation Benchmark

Sitong Su¹ Xiao Cai¹ Lianli Gao¹ Pengpeng Zeng¹ Qinhong Du¹ Mengqi Li¹
 Heng Tao Shen^{1,2} Jingkuan Song^{1*}

¹ University of Electronic Science and Technology of China (UESTC)

² Tongji University

{sitongsu9796, xiaocai628}@gmail.com,

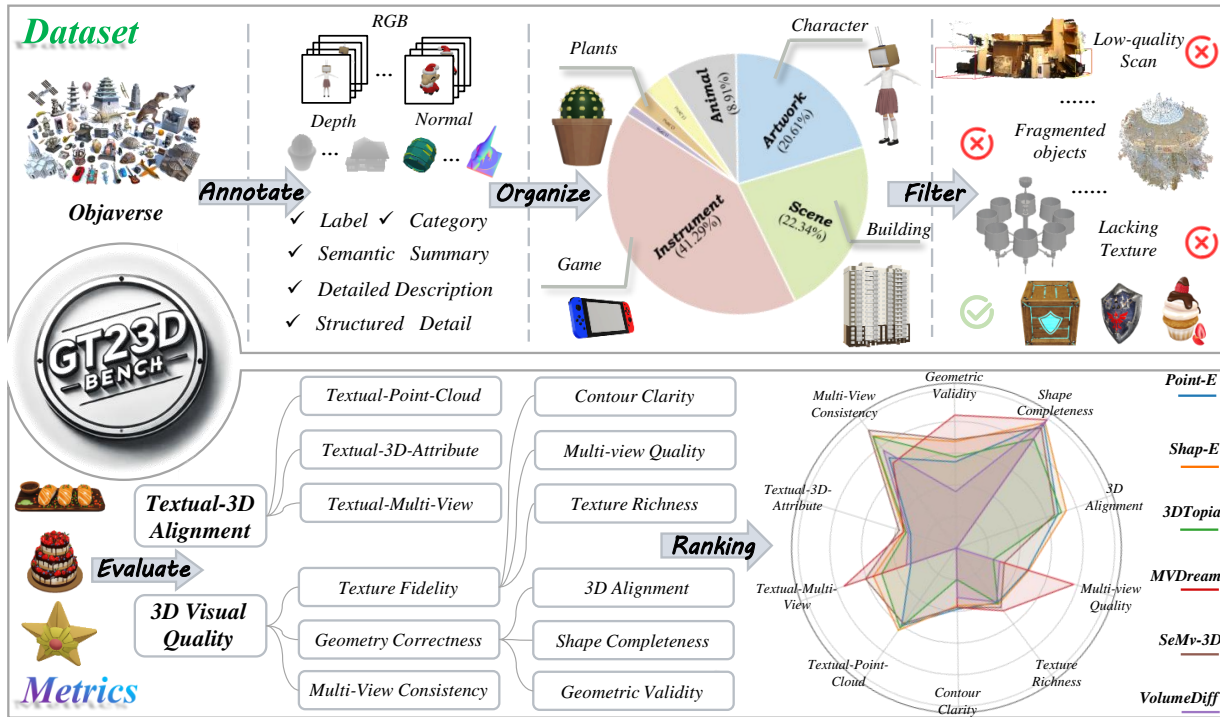


Figure 1. **GT23D-Bench is the first benchmark for General Text-to-3D**, which consists of two components: 1) a 400K multimodal-annotated label-organized thoroughly-filtered 3D Dataset (up) and 2) comprehensive 3D-Aware Evaluation Metrics (down).

Abstract

Recent advances in General Text-to-3D (GT23D) have been significant. However, the lack of a benchmark has hindered systematic evaluation and progress due to issues in datasets and metrics: 1) The largest 3D dataset Objaverse suffers from omitted annotations, disorganization, and low-quality. 2) Existing metrics only evaluate textual-image alignment without considering the 3D-level quality. To this end, we **are the first** to present a comprehensive benchmark for GT23D called GT23D-Bench consisting of: 1) a 400k

high-fidelity and well-organized 3D dataset that curated issues in Objaverse through a systematical annotation-organize-filter pipeline; and 2) comprehensive 3D-aware evaluation metrics which encompass 10 clearly defined metrics thoroughly accounting for multi-dimension of GT23D. Notably, GT23D-Bench features three properties: **1) Multi-modal Annotations.** Our dataset annotates each 3D object with 64-view depth maps, normal maps, rendered images, and coarse-to-fine captions. **2) Holistic Evaluation Dimensions.** Our metrics are dissected into a) Textual-3D Alignment measures textual alignment with multi-granularity vi-

sual 3D representations; and b) 3D Visual Quality which considers texture fidelity, multi-view consistency, and geometry correctness. **3) Valuable Insights.** We delve into the performance of current GT23D baselines across different evaluation dimensions and provide insightful analysis. Extensive experiments demonstrate that our annotations and metrics are aligned with human preferences. Our GitHub is available at <https://gt23d-bench.github.io/>

1. Introduction

General Text-to-3D (GT23D) [1, 2, 9, 14, 18, 32, 42, 44], which generates 3D content from textual descriptions without the need for per-scene optimization, has made remarkable progress in recent years. Despite this progress, a benchmark for GT23D remains absent, which is essential in systematically evaluating and advancing GT23D methods. Specifically, two primary challenges in datasets and metrics currently impede the establishment of the benchmark:

1) Datasets. Objaverse [6], with 800k 3D objects, outpaces other datasets vastly and is widely used in GT23D methods. Nevertheless, it faces three major issues: a) Omitted Annotations: essential annotations like detailed captions or multi-view images are missing. b) Disorganization: due to label misalignment, label absence (52.91%), and semantic overlap (25.93% with 2 labels). c) Low-Quality 3D Shapes: including fragmented objects and low scan quality, lacking texture, and meaningless 3D shapes.

2) Metrics. Existing metrics for GT23D primarily assess 2D-level semantic alignment, such as Clip Scores [10, 38], which measure the similarity between rendered images and input text. However, these metrics overlook critical aspects of text-to-3D generation, particularly in the 3D domain, such as 3D shape correctness.

To address these two issues, we are the first to propose a comprehensive and robust benchmark specifically designed for the GT23D task coined as **GT23D-Bench**, which consists of two main components:

The first component is a **400k multimodal-annotated label-organized thoroughly-filtered 3D Dataset**, carefully curated by addressing Objaverse’s three key issues through a three-staged annotation-organize-filter pipeline. The statistical information comparison with other 3D datasets is shown in Tab. 1. **1)** For the annotation stage named **Multi-Modal Annotations**, to facilitate multi-modal supervision in the 3D generation, we annotated a 3D shape with captions, depth maps, point clouds, and normal maps. For captions, considering different individuals describe a 3D object with different levels of complexity, we introduced coarse-to-fine captions including semantic summaries, detailed descriptions, and structural details, as shown in Fig. 2 a). **2)** For the organize stage named **Label-based Organize**, we first correct misaligned labels by summarizing captions.

Dataset	Object Quantity	Views/Obj	RGB	Depth	Normal	Caption	Detailed Caption
MVImgNet [54]	220k	~ 32	✓	×	×	×	×
Objaverse [6]	818k	-	✓	×	×	×	×
Cap3D [30]	661k	20	✓	×	×	✓	×
3DTopia [13]	120k	-	✓	×	×	✓	×
Ours	400k	64	✓	✓	✓	✓	✓

Table 1. **Statistic comparison of different 3D datasets**, indicating ours features multimodal annotations. “Views/Obj” refers to the number of rendered views for each object.

Then, we create an organized classification with seven primary categories referring to ImageNet [7] categories, using WordNet [47] nodes for subcategories. Finally, we assign the corrected labels into established subcategories by semantics, adding new subcategories as needed. Category distribution visualization is shown in Fig. 2 b) **3)** In the filter stage named **Quality-based Filter**, we remove fragmented shapes by connected component detection, nonsensical 3D shapes through semantic classification, render failures by detecting colors.

The second component of GT23D-Bench is a set of **comprehensive 3D-Aware Evaluation Metrics**. These metrics are divided into two main categories:

1) Textual-Visual Alignment assesses the alignment between textual descriptions and multi-granularity visual representations such as 3D point clouds, multi-view rendered images, and localized attributes.

2) 3D Visual Quality evaluates critical aspects of 3D model quality, including texture fidelity, geometry correctness, and multi-view consistency. **Texture Fidelity** refers to the realism of surface details on a 3D shape from three key aspects: (1) multi-view image quality: aesthetic realism of the texture across different views; (2) contour clarity: judging whether object boundaries remain distinct; and (3) texture richness, gauging the texture details to achieve a lifelike representation. **Geometry Correctness** assesses the structural integrity and physical plausibility of a 3D shape, focusing on (1) semantic alignment with realistic 3D point cloud representations; (2) shape completeness, verifying that models maintain a whole, unfragmented form; and (3) geometric validity, assessing whether the model’s geometry aligns with physical-world constraints. **Multi-view Consistency** For GT23D methods that generate only multi-view images without explicit 3D representations, it is essential to evaluate the visual consistency across different views.

Extensive experiments show that our provided annotations and 3D-aware metrics align better with human perception compared to the current baselines. Using these validated annotations and metrics, we provide a ranked evaluation of current GT23D methods and corresponding analysis.

Our contribution could be summarized as follows:

1). We present **GT23D-Bench**, the *first* benchmark specifically designed for GT23D, consisting of a 400K multimodal-annotated label-organized thoroughly-filtered

3D dataset and a comprehensive suite of 3D-Aware evaluation metrics.

2). We propose a set of holistic evaluation metrics specifically designed for GT23D, which thoroughly capture its multifaceted dimensions and are decomposed into two well-defined components: Textual-3D Alignment and 3D Visual Quality.

3). Extensive experiments verify that our annotations and proposed metrics align closely with human preferences. Accordingly, we provide a ranked evaluation and insightful analysis of current GT23D methods.

2. Related Works

2.1. Text-to-3D Generation

Text-to-3D generation creates 3D representations based on texts, which are classified into: **Per-scene Text-to-3D** generation has primarily been advanced by optimization-based methods like NeRF [31] and 3DGS [19, 34], but lacks zero-shot generalization. Techniques like score distillation [35, 50] employ knowledge in image diffusion to refine 3D models, mitigating over-saturation. Other methods [36, 37] leverage diffusion models fine-tuned on 3D data to handle complex surfaces. **General Text-to-3D** methods enable general generation without per-scene optimization. Early methods like Point-E [32] and Shap-E [18] rely on large 3D datasets to generate point clouds and meshes. Due to the scarcity of 3D data, recent approaches [2, 9, 44] utilize image diffusion models as 2D priors to enhance training and generalization. Inspired by image-to-3D models [25, 26], MVDream [1, 42] jointly trains image generation models with multi-view images, producing diverse object images with competitive results.

2.2. 3D Datasets

Early 3D datasets like ShapeNet [3] contain low-quality, untextured CAD models, while later datasets, such as 3DScan [4], AMTObjects [11], OmniObject3D [52] and MVImgNet [54], provide real-world scans but are limited in scale or quality (e.g., sparse point clouds). Recently, Objaverse [6] introduces a large-scale dataset with many richly textured 3D objects. However, its web-sourced data suffers from coarse or omitted annotations, uneven quality, and labeling errors. Although Objaverse-XL [5] expands to 10 million objects, such issues remain unresolved.

2.3. Text-guided Generation Evaluation

Evaluating text-guided generative models is challenging, yet crucial for assessing their generative capabilities.

Text-to-Image Benchmark Initially, T2I generation is evaluated with metrics like FID [12] and IS [41] compared with ground truth images. However, these metrics fall short in open-domain settings for lack of ground truth images.

Thus, numerous benchmarks [15, 20, 29] now incorporate large multimodal models [33] and advanced tools [21, 57] for more comprehensive assessments.

Text-to-Video Benchmark Similarly, early video generation models use FVD [48], a derivative of FID, for performance evaluation against ground truth data. In open-domain settings, advanced benchmarks [16, 17, 27, 28] now offer holistic evaluations of video performance using pre-trained models, assessing aspects like the temporal consistency, and the quality of motion.

Text-to-3D Benchmark Current text-to-3D evaluations utilize image-level metrics like CLIP score [38] or Aesthetic scores [8], thus overlooking intrinsic 3D features. Though GPTEval3D [51] and T3bench [10] consider holistic dimensions of text-to-3D, they are designed for per-scene methods and require delicate mesh for inputs that cannot be generated by current GT23D methods. Therefore, a more specifically designed benchmark for GT23D is indispensable.

3. 3D Datasets

Objaverse [6] is the largest 3D dataset, widely used by GT23D methods. Yet, it still suffers from issues, including omitted annotations, disorganization, and low-quality 3D shapes. To address these three challenges, we curate Objaverse through a three-stage systematic algorithm consisting of Multi-Modal Annotations 3.1, Label-based Organize 3.2, and Quality-based Filtering 3.3.

3.1. Multi-Modal Annotations

We provide Objaverse with multimodal annotations to facilitate paired data supervision in GT23D training and evaluation. For vision annotation, we uniformly sample [43] 64 multi-view RGB images by rotating around the azimuth angle at 360 degrees within three elevation intervals: 0 degrees, 30 degrees, and 60 to 90 degrees. In addition, we annotate depth maps, normal maps, and camera parameters corresponding to these views.

For caption annotation, we implement a multi-level approach to accommodate varying levels of descriptive detail. Specifically, we enable the pre-trained multimodal model LLaVA [24] to caption a 3D object from its rendered three views (front, side, and back) with increasing levels of detail. As shown in Fig. 2 a), the final caption includes a Label, a Semantic Summary, and two Detailed Descriptions from different angles, covering both part attributes and relationships between parts. Furthermore, for efficient detail extraction from captions, we leverage the pre-trained large language model LLaMA [45] to convert detailed descriptions into structured details in a dictionary format (e.g., Shirt: white collar, ...), as illustrated in Fig. 2 a).

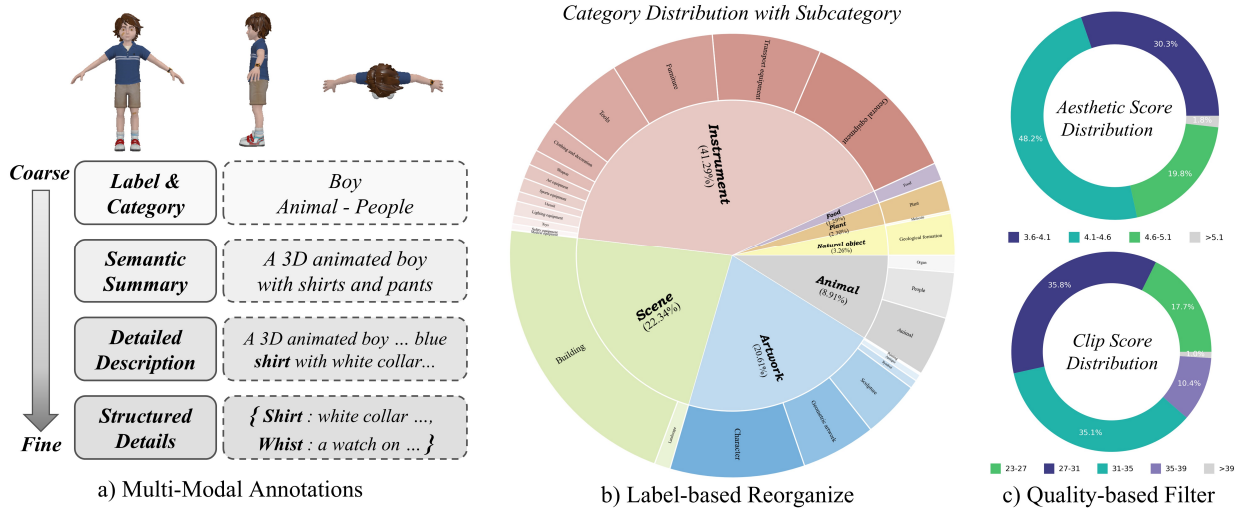


Figure 2. **Statistic information of our 3D dataset.** In a) *Multi-Modal Annotations*, we demonstrate an example with coarse-to-fine captions using algorithms in Sec. 3.1. In b) *Label-based Organize*, distributions of seven categories with their subcategories through algorithms in Sec 3.2 are visualized. In c) *Quality-based Filter*, We show the distribution of Clip and Aesthetic scores after filtering in Sec 3.3, which ensures a certain level of textual-visual alignment and visual aesthetic quality.

3.2. Label-based Organize

To address the dataset disorganization caused by label misalignment, label absence, and semantic overlap (with two labels), we implement a systematic approach during the Label-based Organization stage.

To ensure accurate label semantics, we first use the large language model LLaMA [45] to extract the main subject from each generated caption (e.g., “dinosaur” from “A green dinosaur with a gray pedestal”). We then classify these labels into seven primary categories—scene, instrument, plant, food, animal, artwork, and natural object—designed to align with ImageNet’s structure [7]. For each category, we identify subcategories using WordNet [47] and select appropriate sub-nodes. Following this hierarchy, we assign each label to a primary category and its relevant subcategory, leveraging LLaMA [45] to generate new subcategories as needed, ensuring comprehensive dataset organization.

3.3. Quality-based Filter

Objaverse suffers from fragmented objects and low scan quality, lacking texture, and meaningless 3D shapes. To address this, we design a series of filtering algorithms.

For fragmented object removal, we analyze connected components in rendered images, flagging objects as noisy if isolated components smaller than 10 pixels constitute over 1% of the object’s area. We then filter out objects lacking texture or with failed renders, detected by identifying images where all RGB values are gray. To further refine the

dataset, we apply the multimodal model LLaMA [45] to exclude unrecognizable and meaningless objects by assessing multi-view images with their captions for real-world associations. Lastly, to ensure high textual-visual alignment and aesthetic quality, we calculate the CLIP Score and Aesthetic Score for each object, filtering out those scoring below 20% for CLIP and 30% for aesthetics. The resulting statistics are shown on the right of Fig. 2.

4. 3D-Aware Evaluation Metrics

For a comprehensive evaluation of GT23D, we divide text-to-3D generation quality into two vital and orthogonal components. First, we focus on Textual-3D Alignment in 4.1, evaluating how well the generated 3D models align with the textual descriptions. Second, we assess the 3D Visual Quality in 4.2 by examining determining factors of 3D shapes including texture, geometry, and multi-view consistency.

During the evaluation, given a textual description \mathcal{T} and a GT23D generation model G , we obtain the generated 3D representation $G(\mathcal{T})$. Then we render an image I every 30° and obtain a total of 12 multiview images I_{mv} , and extract the corresponding point clouds P . The evaluation is then carried out based on the following criteria.

4.1. Textual-3D Alignment

To thoroughly evaluate Textual-3D alignment, we consider the alignment between text and various levels of 3D representation, from high-level semantics to detailed fea-

tures. These representations include point clouds (4.1.1), multi-view images (4.1.1), and attributes (4.1.3).

4.1.1 Textual-Point Cloud Alignment (T-PC)

A global evaluation from the 3D shape offers a more comprehensive assessment compared to evaluating features from rendered images alone. Given the diverse 3D outputs of different methods, we standardize them by converting their outputs to point clouds. Utilizing open domain text-point-cloud model Uni3D [56], we extract visual features from the point cloud P and compute their similarity to textual features from prompt \mathcal{T} , which is expressed as:

$$Score_{T-PC} = Uni3D(\mathcal{T}, P). \quad (1)$$

4.1.2 Textual-Multiview Alignment (T-MV)

Although the Clip Score is designed to assess textual-image alignment, it primarily evaluates global alignment, often overlooking fine-grained details. To address this limitation, we leverage VQAScore [22], which is particularly effective at processing compositional text prompts with details. By inputting text \mathcal{T} and multiview images I_{mv} into VQAScore we calculate Textual-Multiview Alignment as:

$$Score_{T-MV} = VQAScore(\mathcal{T}, I_{mv}). \quad (2)$$

4.1.3 Textual-3D Attribute Alignment(T-Attr)

To verify the precise semantic alignment of generated results, we also analyze semantics from a finer-grained local component perspective. In practice, we employ attributes in input prompts to localize and detect corresponding components across multiple views, using Grounded-SAM [39]. Then, we calculate the detection confidence ($conf_i$) and probability ($prob_i$) for each attribute i to evaluate whether all N components are detected and how well they align with the specified attributes. Finally, $conf_i$ and $prob_i$ are jointly combined to form the final score $Score_{T-Attr}$:

$$Score_{T-Attr} = \frac{1}{N} \sum_{i=1}^N conf_i \times prob_i. \quad (3)$$

4.2. 3D Visual Quality

We decompose and evaluate a 3D shape quality from two vital components: texture and geometry. The texture encapsulates the surface appearance of a 3D object 4.2.1. Differently, geometry defines the overall structure and shape of the object 4.2.2. Additionally, for the GT23D methods that only generate multi-view images, it is also crucial to evaluate the correspondence among different views 4.2.3.

4.2.1 Texture Fidelity

1.Multi-view Image Quality (MV-IQ) evaluates the overall quality of rendered images across multiple views of a 3D shape, including aesthetic factors and the degree of alignment with real-world geometry. In practice, we employ a powerful image quality assessment model, LIQE [55], to score the multi-view images MV :

$$Score_{MV-IQ} = LIQE(I_{mv}). \quad (4)$$

2.Contour Clarity (CC) assesses the clarity and definition of object contours and edges, determining the presence of blurring or noise in the generated 3D model.

To evaluate the clarity of generated images, we propose a re-blur evaluation strategy inspired by super-resolution. In this approach, we apply a Gaussian blur filter to the original image I , producing a blurred version I_{blur} . The assessment score is based on the degree of change in sharpness between I and I_{blur} . To quantify the sharpness, we measure the variation in pixel intensity gradients across the image for I and I_{blur} , which are respectively denoted as S and S_{blur} . By comparing the sharpness of I and I_{blur} and normalizing this difference, we obtain a final clarity score that reflects the fidelity of the generated image:

$$Score_{CC} = \frac{S - S_{blur}}{S}. \quad (5)$$

3.Texture Richness (TR) evaluates how well the textures capture details and realism. To determine whether an object is texture-rich, we leverage the powerful capabilities of the pre-trained image generation model, Stable Diffusion [40]. By applying an inversion process [46], we map a rendered image I back into the noise space, allowing Stable Diffusion to regenerate the image based on the inverted noise.

Subsequently, we assess texture richness by comparing the texture details of the regenerated image I_{inv} with the original image I . Specifically, we utilize a canny edge density metric $Ced(\cdot)$ to capture the level of detail. Thus, the texture richness score is defined as:

$$Score_{TR} = \frac{Ced(I)}{Ced(I) + Ced(I_{inv})}. \quad (6)$$

4.2.2 Geometry Correctness

To evaluate Geometry Correctness, we focus on three core aspects that ensure the structural integrity and logical coherence of 3D shapes.

1.3D Alignment (3D-Ali) To evaluate whether the generated 3D representations align with real-world distributions, we measured the feature-space distance between generated and real 3D representations. Specifically, we employ Uni3D [56], a pre-trained cross-modal 3D-text alignment model, to extract 3D features for both generated point

		Textual Point-Cloud	Textual Multi-View	Textual 3D-Attribute	Texture Fidelity			Geometry Correctness			Multi-View Consistency
					Mv-IQ	CC	TR	3D-Ali	Shape-C	Geo-V	
Person (ρ) \uparrow	Clip Score	0.2077	0.2077	0.2077	0.2077	0.2077	0.2077	0.2077	0.2077	0.2077	0.2077
	Aesthetic Score	0.2619	0.2619	0.2619	0.2619	0.2619	0.2619	0.2619	0.2619	0.2619	0.2619
	Ours	0.4238	0.4536	0.4598	0.4229	0.5745	0.4663	0.6645	0.5058	0.4557	0.4544
Spearsman (ρ) \uparrow	Clip Score	0.2008	0.2008	0.2008	0.2008	0.2008	0.2008	0.2008	0.2008	0.2008	0.2008
	Aesthetic Score	0.3265	0.3265	0.3265	0.3265	0.3265	0.3265	0.3265	0.3265	0.3265	0.3265
	Ours	0.4436	0.3680	0.4241	0.5309	0.6778	0.4081	0.6446	0.4693	0.4585	0.5186
Kendall (τ) \uparrow	Clip Score	0.1528	0.1528	0.1528	0.1528	0.1528	0.1528	0.1528	0.1528	0.1528	0.1528
	Aesthetic Score	0.2153	0.2153	0.2153	0.2153	0.2153	0.2153	0.2153	0.2153	0.2153	0.2153
	Ours	0.3288	0.2630	0.3332	0.4270	0.5613	0.3254	0.4932	0.3951	0.3691	0.3971

Table 2. **Human alignment comparison across different GT23D evaluation metrics considering different evaluation dimensions.** Correlation coefficient Pearson’s ρ , Spearman’s ρ , and Kendall’s τ evaluate correlations between human scores and metric scores.

clouds P_g and ground truth point clouds P_{gt} from real objects and then compute their cosine similarity.

$$Score_{3D-Ali} = \text{Cosine}(\text{Uni3D}(P_g), \text{Uni3D}(P_{gt})) \quad (7)$$

2. Shape Completeness (Shape-C) verifies for the integrity of the shape. Concretely, if two regions lack directly connected colored pixels, they are considered separate connected components. If the area of a connected component is smaller than a threshold (in pixels), it is considered a fragment, with area S_{frag} . The ratio of the total area of all fragments to the object’s total area S_{obj} reflects the shape completeness.

$$Score_{Shape-C} = 1 - \frac{\sum S_{frag}}{S_{obj}} \quad (8)$$

3. Geometric Validity (Geo-V) To assess the geometric quality and realism of 3D models, we prompt GPT [33] with multi-view rendered images and request scoring based on three criteria: geometric accuracy, alignment with textual description, and geometric quality.

First, for geometric accuracy, GPT evaluates whether model structures are realistic and obey physical rules $Score_1$. Second, in alignment with textual description, GPT assesses whether the model’s shape intuitively reflects its described object class $Score_2$. Finally, for geometric quality, GPT evaluates 3D coherence by identifying issues such as fragmentation, and disjointed parts $Score_3$. Ultimately, the three scores are averaged to determine the model’s geometric validity:

$$Score_{Geo-V} = \text{Average}(Score_1, Score_2, Score_3) \quad (9)$$

4.2.3 Multi-View Consistency

We leverage the pre-trained model DepthAnything [53] to estimate depth maps for multi-view images, which enables

	Objaverse	Cap3D	3DTopia	Ours
Human Alignment \uparrow	2.34	3.11	3.50	3.89
Training Boost \uparrow	2.81	3.68	3.85	4.28

Table 3. Comparisons of Objaverse, Cap3D, 3DTopia, and Ours on dataset captions quality. **Human Alignment** refers to human preference on captions quality. **Training Boost** shows human preference on the performance of a GT23D method training with captions from different baselines.

us to project images from a source view back into 3D space as point clouds. Using the camera parameters for the target view, we then re-render this point cloud as an image $I_{re-render}$. Despite some loss of 3D content, the core color distribution and contour shapes remain intact. By comparing the re-rendered image $I_{re-render}$ with the target view image I_{tar} , we can evaluate the visual similarity of the object between the source view and target view with image metrics like SSIM [49], thereby assessing the coherence of the multi-view generation.

$$Score_{MV-Con} = \text{SSIM}(I_{re-render}, I_{tar}) \quad (10)$$

5. Experiments

5.1. Experimental Setup

GT23D Baselines. We select baseline methods from two categories defined in [2] within the open-source GT23D methods. The *finetune-based methods*, including MVDream [42], generate only multi-view images and do not produce actual 3D representations. The *prior-based methods*, including Point-E, Shap-E, VolumeDiffusion, 3DTopia, and SeMv-3D [2, 18, 32, 44], can generate explicit or implicit 3D representations. For each method, we use the official test scripts to generate the 3D results.

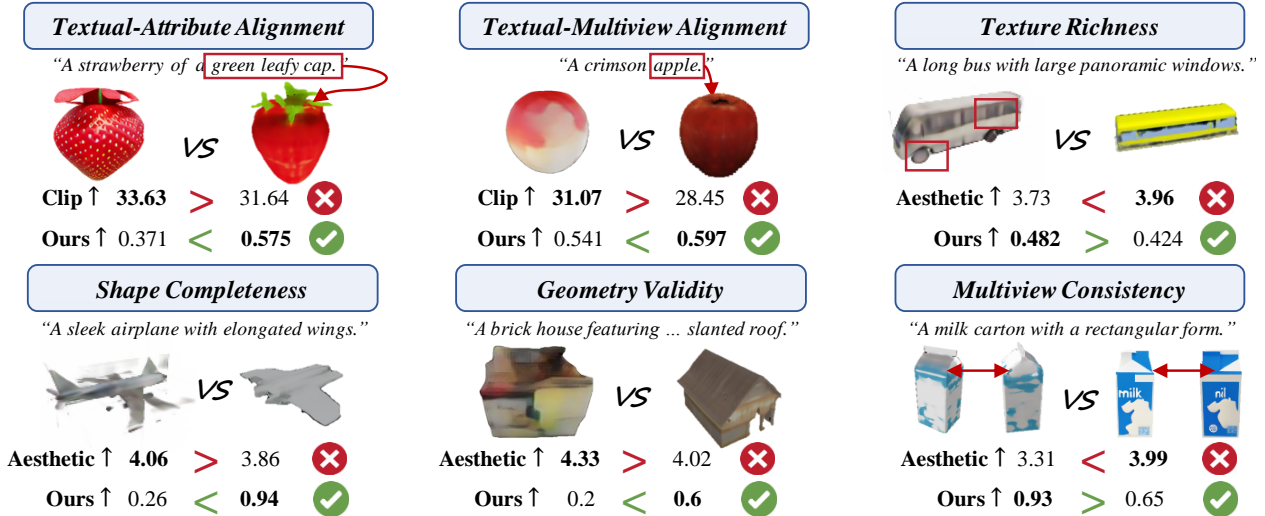


Figure 3. Visual analysis comparing GT23D metrics including Clip Scores (Clip), Aesthetic Scores (Aesthetic), and Ours considering different evaluation dimensions. Our evaluation scores are better consistent with visual results in each evaluation dimension.

Metric Baselines. Compared metric baselines include *Clip Score* [38] which are commonly used in previous works [2, 14, 18, 32, 42, 44] to assess textual-3D alignment. *Aesthetic Scores* [8] evaluate rendered multiview image quality from an aesthetic perspective.

Prompt Construction For *ground truth evaluation*, we randomly sample 30 captions from our proposed datasets in each of the primary categories, for a total of 180 prompts. For *open-domain evaluation*, GPT [33] is utilized to create 200 prompts considering different degrees of prompt complexity and imaginativeness. Details refer to Appendix.

5.2. Comparison on Datasets Captions

Human Alignment Comparison. To demonstrate captions in our dataset better reflect human expressions, we conduct a user study comparing different caption methods on Objaverse as shown in the first row of Tab. 3. We invite 40 users to score caption quality from 1 to 5, collecting a total of 1600 scores. As shown in Tab. 3, our method significantly outperforms other caption methods on Objaverse in terms of human alignment.

Training Boost Comparison. To validate that our annotated captions could better promote training effectiveness of GT23D methods, we finetune the same GT23D model called SeMV-3D using captions from Objaverse, Cap3D, 3DTopia, and Ours. Then 40 users are invited to score the generation visual results of the four baselines from 1 to 5, which are shown in the second row of 3. As observed, finetuned results using our captions received the highest score of 4.28, which verifies that our captions demonstrate better quality thus aiding generation training better.

5.3. Comparison on Metrics

Human Alignment Comparison. We conduct a user study to verify the reliability of our metrics compared to Clip and Aesthetic Scores. Expert users rate results from six GT23D baselines, yielding 5040 scores. We then calculate the correlation between these human scores and metric scores using Pearson’s ρ , Spearman’s ρ , and Kendall’s τ , as shown in Tab. 2. As seen, our metrics show significantly stronger correlations across all 10 evaluation dimensions considering different aspects of text-to-3D quality.

Visual Comparison. For further validation of our metrics superiority from visual aspects, we compare visual results with scores from Clip Score (Clip), Aesthetic Score (Aesthetic), and ours in Fig. 3. As seen, our scores remain more consistent with visual quality in different evaluation dimensions compared to Clip and Aesthetic. For example, in “Multiview Consistency” in the bottom-right corner, the Aesthetic favors a view-inconsistent method due to better visual appeal, while our metrics more accurately reflect view consistency, providing a fairer assessment.

To verify that our metrics could reflect variations, we raise two visual examples in Fig. 5 considering “Texture Richness” and “Shape Completeness”. For the example in the bottom row of Fig. 5, as the outlier noises gradually decrease from left to right, our scores evaluating shape completeness respectively increase.

5.4. Comparisons across GT23D methods

As shown in Tab. 5 and Fig. 4, we conduct a comprehensive evaluation of existing GT23D models using our GT23D-Bench metrics from six main dimensions containing 10 metrics in total. Accordingly, we provide insightful

	Textual-PointCloud	Textual-MultiView	Textual-Attribute	Texture Fidelity			Geometry Correctness			Multi-View Consistency
				CC	TR	Mv-IQ	3D-Ali	Shape-C	Geo-V	
Point-E	0.6017	0.3041	0.3039	0.3867	0.4314	0.4706	0.6787	0.9564	0.5447	0.7121
Shap-E	0.6364	0.5543	0.3478	0.3646	0.4425	0.4777	0.7322	0.9707	0.6733	0.8845
VolumeDiffusion	-	0.3188	0.3347	0.3127	0.4245	0.2962	-	0.9878	0.3567	0.7714
3DTopia	0.6184	0.4989	0.3327	0.1995	0.4381	0.2438	0.7008	0.8458	0.5753	0.8801
SeMv-3D	0.5838	0.6068	0.3791	0.3747	0.4698	0.3157	0.6544	0.9291	0.686	0.9293
MVDream	-	0.7510	0.3487	0.3759	0.4951	0.7753	-	0.9922	0.84	0.6698

Table 4. **Quantitative comparison of different GT23D baselines using metrics of GT23D-Bench in 10 different evaluation dimensions.** The higher scores indicate better performance. Since VolumeDiffusion and MVDream do not output explicit 3D representations, their scores are absent in Textual-PointCloud and 3D-Ali which need point clouds.

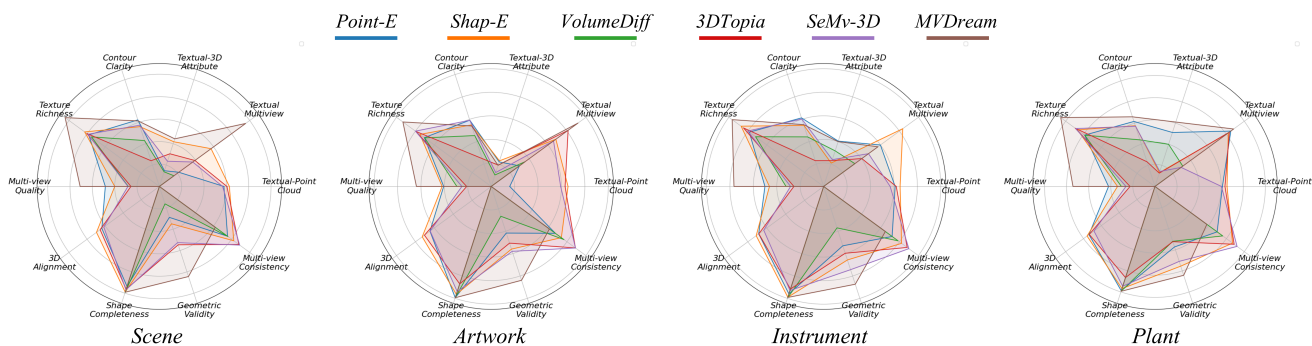


Figure 4. **Plot visualization** of quantitative comparisons on GT23D baselines using metrics of GT23D-Bench across four content categories. Additional plot results refer to Appendix.

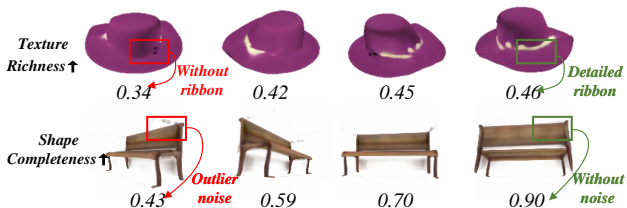


Figure 5. Visual examples demonstrating our metrics' ability to reflect variations in "Texture Richness" and "Shape Completeness."

observations in GT23D methods as follows.

Existing methods align with overall semantics but struggle with generating fine details. Even fine-tune-based approaches like MVDream, which utilizes pre-trained models, still produce errors in component and detail generation. We speculate that this is primarily due to the lack of high-quality text-to-3D datasets. In support of this, our experiments in Tab. 3 show that models trained with high-quality captions exhibit better semantic understanding, underscoring the crucial need for high-quality 3D datasets to improve GT23D in the future.

Different output 3D representations significantly impact GT23D quality. Multi-view image-based methods like MVDream achieve high visual quality in single-view images (high Texture Fidelity score) but lack 3D supervision, resulting in poor 3D quality (low Multi-View Consistency score). In contrast, explicit 3D representations like Point-E improve 3D semantic accuracy (high Textual-Point Cloud score) through 3D supervision, but this coarse supervision leads to noise and texture issues. Different from the former two, Shap-E, using implicit 3D representations, balances 3D semantics and detail quality, excelling across multiple evaluation metrics.

Emphasis on generalization in GT23D methods leads to a decline in generation stability. Methods that output 3D representations often struggle with generative success rates, particularly for complex artwork or large-scale scenes requiring substantial 3D structure for accurate depiction and control, as shown in Fig. 4. These methods frequently need multiple attempts to produce satisfactory results, leading to poor overall performance.

Effective preservation and utilization of image prior knowledge remain pressing challenges. Methods like

MVDream have indicated that existing pretrained text-to-image generation models could provide sufficient prior knowledge for multi-view 3D generation. However, for methods that generate explicit 3D representations, even when leveraging similar powerful pre-trained image priors, the results remain suboptimal. We propose that this is due to a knowledge drift from pretrained text-to-image space to the 3D representation space, causing the 3D generation models to forget certain features within prior knowledge.

6. Conclusion

We introduce the first benchmark for GT23D, addressing issues in datasets and evaluation metrics. By creating a 400k multimodal annotated 3D dataset, we enhance Objaverse and ensure high quality and organization. Our 3D-aware Evaluation Metrics offer a deeper assessment of Textual-3D Alignment and 3D Visual Quality. Experiments confirm that our benchmark aligns closely with human judgment.

References

- [1] Andreas Blattmann, Tim Dockhorn, Sumith Kulal, Daniel Mendelevitch, Maciej Kilian, Dominik Lorenz, Yam Levi, Zion English, Vikram Voleti, Adam Letts, Varun Jampani, and Robin Rombach. Stable video diffusion: Scaling latent video diffusion models to large datasets. *arXiv*, 2023. [2](#), [3](#)
- [2] Xiao Cai, Pengpeng Zeng, Lianli Gao, Junchen Zhu, Jiaxin Zhang, Sitong Su, Heng Tao Shen, and Jingkuan Song. Semv-3d: Towards semantic and multi-view consistency simultaneously for general text-to-3d generation with triplane priors. *arXiv preprint arXiv:2410.07658*, 2024. [2](#), [3](#), [6](#), [7](#), [12](#)
- [3] Angel X. Chang, Thomas A. Funkhouser, Leonidas J. Guibas, Pat Hanrahan, Qi-Xing Huang, Zimo Li, Silvio Savarese, Manolis Savva, Shuran Song, Hao Su, Jianxiong Xiao, Li Yi, and Fisher Yu. Shapenet: An information-rich 3d model repository. *arXiv*, 2015. [3](#)
- [4] Sungjoon Choi, Qian-Yi Zhou, Stephen Miller, and Vladlen Koltun. A large dataset of object scans. *arXiv*, 2016. [3](#)
- [5] Matt Deitke, Ruoshi Liu, Matthew Wallingford, Huong Ngo, Oscar Michel, Aditya Kusupati, Alan Fan, Christian Laforte, Vikram Voleti, Samir Yitzhak Gadre, Eli VanderBilt, Aniruddha Kembhavi, Carl Vondrick, Georgia Gkioxari, Kiana Ehsani, Ludwig Schmidt, and Ali Farhadi. Objaverse-xl: A universe of 10m+ 3d objects. *arXiv preprint arXiv:2307.05663*, 2023. [3](#)
- [6] Matt Deitke, Dustin Schwenk, Jordi Salvador, Luca Weihs, Oscar Michel, Eli VanderBilt, Ludwig Schmidt, Kiana Ehsani, Aniruddha Kembhavi, and Ali Farhadi. Objaverse: A universe of annotated 3d objects. In *CVPR*, pages 13142–13153, 2023. [2](#), [3](#), [12](#)
- [7] Jia Deng, Wei Dong, Richard Socher, Li-Jia Li, Kai Li, and Li Fei-Fei. Imagenet: A large-scale hierarchical image database. In *CVPR*, 2009. [2](#), [4](#), [12](#)
- [8] Grexzen. Sd-chad, 2024. [3](#), [7](#)
- [9] Anchit Gupta, Wenhan Xiong, Yixin Nie, Ian Jones, and Barlas Oguz. 3dgen: Triplane latent diffusion for textured mesh generation. *arXiv*, 2023. [2](#), [3](#)
- [10] Yuze He, Yushi Bai, Matthieu Lin, Wang Zhao, Yubin Hu, Jenny Sheng, Ran Yi, Juanzi Li, and Yong-Jin Liu. T bench: Benchmarking current progress in text-to-3d generation. *arXiv preprint arXiv:2310.02977*, 2023. [2](#), [3](#)
- [11] Philipp Henzler, Jeremy Reizenstein, Patrick Labatut, Roman Shapovalov, Tobias Ritschel, Andrea Vedaldi, and David Novotný. Unsupervised learning of 3d object categories from videos in the wild. In *CVPR*, pages 4700–4709, 2021. [3](#)
- [12] Martin Heusel, Hubert Ramsauer, Thomas Unterthiner, Bernhard Nessler, and Sepp Hochreiter. Gans trained by a two time-scale update rule converge to a local nash equilibrium. *NeurIPS*, 2017. [3](#)
- [13] Fangzhou Hong, Jiayang Tang, Ziang Cao, Min Shi, Tong Wu, Zhaoxi Chen, Tengfei Wang, Liang Pan, Dahua Lin, and Ziwei Liu. 3dtopia: Large text-to-3d generation model with hybrid diffusion priors. *arXiv*, 2024. [2](#)
- [14] Fangzhou Hong, Jiayang Tang, Ziang Cao, Min Shi, Tong Wu, Zhaoxi Chen, Shuai Yang, Tengfei Wang, Liang Pan,

- Dahua Lin, et al. 3dtopia: Large text-to-3d generation model with hybrid diffusion priors. *arXiv preprint arXiv:2403.02234*, 2024. 2, 7, 12
- [15] Kaiyi Huang, Kaiyue Sun, Enze Xie, Zhenguo Li, and Xihui Liu. T2i-compbench: A comprehensive benchmark for open-world compositional text-to-image generation. *NeurIPS*, 2023. 3
- [16] Ziqi Huang, Yanan He, Jiashuo Yu, Fan Zhang, Chenyang Si, Yuming Jiang, Yuanhan Zhang, Tianxing Wu, Qingyang Jin, Nattapol Chanpaisit, et al. Vbench: Comprehensive benchmark suite for video generative models. In *CVPR*, 2024. 3
- [17] Pengliang Ji, Chuyang Xiao, Huilin Tai, and Mingxiao Huo. T2vbench: Benchmarking temporal dynamics for text-to-video generation. In *Proceedings of the IEEE/CVF Conference on Computer Vision and Pattern Recognition*, pages 5325–5335, 2024. 3
- [18] Heewoo Jun and Alex Nichol. Shap-e: Generating conditional 3d implicit functions. *arXiv*, 2023. 2, 3, 6, 7, 21
- [19] Bernhard Kerbl, Georgios Kopanas, Thomas Leimkühler, and George Drettakis. 3d gaussian splatting for real-time radiance field rendering. *ACM Trans. Graph.*, 2023. 3
- [20] Baiqi Li, Zhiqiu Lin, Deepak Pathak, Jiayao Emily Li, Xide Xia, Graham Neubig, Pengchuan Zhang, and Deva Ramanan. Genai-bench: A holistic benchmark for compositional text-to-visual generation. In *Synthetic Data for Computer Vision Workshop @ CVPR 2024*, 2024. 3
- [21] Junnan Li, Dongxu Li, Caiming Xiong, and Steven Hoi. Blip: Bootstrapping language-image pre-training for unified vision-language understanding and generation. In *ICML*. PMLR, 2022. 3
- [22] Zhiqiu Lin, Deepak Pathak, Baiqi Li, Jiayao Li, Xide Xia, Graham Neubig, Pengchuan Zhang, and Deva Ramanan. Evaluating text-to-visual generation with image-to-text generation. *arXiv preprint arXiv:2404.01291*, 2024. 5
- [23] Haotian Liu, Chunyuan Li, Yuheng Li, Bo Li, Yuanhan Zhang, Sheng Shen, and Yong Jae Lee. Llava-next: Improved reasoning, ocr, and world knowledge. *arXiv*, 2024. 12
- [24] Haotian Liu, Chunyuan Li, Qingyang Wu, and Yong Jae Lee. Visual instruction tuning. In *NeurIPS*, 2023. 3
- [25] Minghua Liu, Chao Xu, Haian Jin, Linghao Chen, Mukund Varma T, Zexiang Xu, and Hao Su. One-2-3-45: Any single image to 3d mesh in 45 seconds without per-shape optimization. In *NeurIPS*, 2023. 3
- [26] Ruoshi Liu, Rundi Wu, Basile Van Hoorick, Pavel Tokmakov, Sergey Zakharov, and Carl Vondrick. Zero-1-to-3: Zero-shot one image to 3d object. In *ICCV*, pages 9264–9275, 2023. 3
- [27] Yaofang Liu, Xiaodong Cun, Xuebo Liu, Xintao Wang, Yong Zhang, Haoxin Chen, Yang Liu, Tiejong Zeng, Raymond Chan, and Ying Shan. Evalcrafter: Benchmarking and evaluating large video generation models. In *CVPR*, 2024. 3
- [28] Yuanxin Liu, Lei Li, Shuhuai Ren, Rundong Gao, Shicheng Li, Sishuo Chen, Xu Sun, and Lu Hou. Fetv: A benchmark for fine-grained evaluation of open-domain text-to-video generation. *NeurIPS*, 2024. 3
- [29] Yujie Lu, Xianjun Yang, Xiujun Li, Xin Eric Wang, and William Yang Wang. Llm-score: Unveiling the power of large language models in text-to-image synthesis evaluation. *NeurIPS*, 2024. 3
- [30] Tiange Luo, Chris Rockwell, Honglak Lee, and Justin Johnson. Scalable 3d captioning with pretrained models. In *NeurIPS*, 2023. 2, 12
- [31] Ben Mildenhall, Pratul P. Srinivasan, Matthew Tancik, Jonathan T. Barron, Ravi Ramamoorthi, and Ren Ng. Nerf: Representing scenes as neural radiance fields for view synthesis. In *ECCV*, pages 405–421, 2020. 3
- [32] Alex Nichol, Heewoo Jun, Prafulla Dhariwal, Pamela Mishkin, and Mark Chen. Point-e: A system for generating 3d point clouds from complex prompts. *arXiv*, 2022. 2, 3, 6, 7, 21
- [33] OpenAI. Gpt-4 technical report, 2023. 3, 6, 7, 24
- [34] Phu Pham, Aradhya N Mathur, Ojaswa Sharma, and Aniket Bera. Mvgaussian: High-fidelity text-to-3d content generation with multi-view guidance and surface densification. *arXiv preprint arXiv:2409.06620*, 2024. 3
- [35] Ben Poole, Ajay Jain, Jonathan T. Barron, and Ben Mildenhall. Dreamfusion: Text-to-3d using 2d diffusion. In *ICLR*, 2023. 3
- [36] Guocheng Qian, Jinjie Mai, Abdullah Hamdi, Jian Ren, Aliaksandr Siarohin, Bing Li, Hsin-Ying Lee, Ivan Skokhodov, Peter Wonka, Sergey Tulyakov, and Bernard Ghanem. Magic123: One image to high-quality 3d object generation using both 2d and 3d diffusion priors. *arXiv*, 2023. 3
- [37] Lingteng Qiu, Guanying Chen, Xiaodong Gu, Qi Zuo, Mutian Xu, Yushuang Wu, Weihao Yuan, Zilong Dong, Liefeng Bo, and Xiaoguang Han. Richdreamer: A generalizable normal-depth diffusion model for detail richness in text-to-3d. *arXiv*, 2023. 3
- [38] Alec Radford, Jong Wook Kim, Chris Hallacy, Aditya Ramesh, Gabriel Goh, Sandhini Agarwal, Girish Sastry, Amanda Askell, Pamela Mishkin, Jack Clark, Gretchen Krueger, and Ilya Sutskever. Learning transferable visual models from natural language supervision. In *ICML*, volume 139, pages 8748–8763, 2021. 2, 3, 7
- [39] Tianhe Ren, Shilong Liu, Ailing Zeng, Jing Lin, Kunchang Li, He Cao, Jiayu Chen, Xinyu Huang, Yukang Chen, Feng Yan, Zhaoyang Zeng, Hao Zhang, Feng Li, Jie Yang, Hongyang Li, Qing Jiang, and Lei Zhang. Grounded sam: Assembling open-world models for diverse visual tasks, 2024. 5, 21
- [40] Robin Rombach, Andreas Blattmann, Dominik Lorenz, Patrick Esser, and Björn Ommer. High-resolution image synthesis with latent diffusion models. In *Proceedings of the IEEE/CVF conference on computer vision and pattern recognition*, pages 10684–10695, 2022. 5, 22, 30
- [41] Tim Salimans, Ian Goodfellow, Wojciech Zaremba, Vicki Cheung, Alec Radford, and Xi Chen. Improved techniques for training gans. *Advances in neural information processing systems*, 29, 2016. 3
- [42] Yichun Shi, Peng Wang, Jianglong Ye, Mai Long, Kejie Li, and Xiao Yang. Mvdream: Multi-view diffusion for 3d generation. *arXiv*, 2023. 2, 3, 6, 7, 21

- [43] C. Bane Sullivan and Alexander A. Kaszynski. Pyvista: 3d plotting and mesh analysis through a streamlined interface for the visualization toolkit (vtk). *Journal of Open Source Software*, 4(37):1450, 2019. 3
- [44] Zhicong Tang, Shuyang Gu, Chunyu Wang, Ting Zhang, Jianmin Bao, Dong Chen, and Baining Guo. Volumediffusion: Flexible text-to-3d generation with efficient volumetric encoder. *arXiv*, 2023. 2, 3, 6, 7, 21
- [45] Hugo Touvron, Thibaut Lavril, Gautier Izacard, Xavier Martinet, Marie-Anne Lachaux, Timothée Lacroix, Baptiste Rozière, Naman Goyal, Eric Hambro, Faisal Azhar, et al. Llama: Open and efficient foundation language models. *arXiv preprint arXiv:2302.13971*, 2023. 3, 4, 12
- [46] Linoy Tsaban and Apolinário Passos. Ledits: Real image editing with ddpm inversion and semantic guidance, 2023. 5, 22
- [47] Princeton University. Wordnet: A lexical database for english, n.d. 2, 4, 12
- [48] Thomas Unterthiner, Sjoerd Van Steenkiste, Karol Kurach, Raphael Marinier, Marcin Michalski, and Sylvain Gelly. Towards accurate generative models of video: A new metric & challenges. *arXiv preprint arXiv:1812.01717*, 2018. 3
- [49] Zhou Wang, Alan C Bovik, Hamid R Sheikh, and Eero P Simoncelli. Image quality assessment: from error visibility to structural similarity. *IEEE transactions on image processing*, 13(4):600–612, 2004. 6
- [50] Zhengyi Wang, Cheng Lu, Yikai Wang, Fan Bao, Chongxuan Li, Hang Su, and Jun Zhu. Prolificdreamer: High-fidelity and diverse text-to-3d generation with variational score distillation. In *NeurIPS*, 2023. 3
- [51] Tong Wu, Guandao Yang, Zhibing Li, Kai Zhang, Ziwei Liu, Leonidas Guibas, Dahua Lin, and Gordon Wetzstein. Gpt-4v (ision) is a human-aligned evaluator for text-to-3d generation. In *CVPR*, 2024. 3
- [52] Tong Wu, Jiarui Zhang, Xiao Fu, Yuxin Wang, Liang Pan Jiawei Ren, Wayne Wu, Lei Yang, Jiaqi Wang, Chen Qian, Dahua Lin, and Ziwei Liu. Omniobject3d: Large-vocabulary 3d object dataset for realistic perception, reconstruction and generation. In *IEEE/CVF Conference on Computer Vision and Pattern Recognition (CVPR)*, 2023. 3
- [53] Lihe Yang, Bingyi Kang, Zilong Huang, Zhen Zhao, Xiaogang Xu, Jiashi Feng, and Hengshuang Zhao. Depth anything v2. *arXiv:2406.09414*, 2024. 6, 24
- [54] Xianggang Yu, Mutian Xu, Yidan Zhang, Haolin Liu, Chongjie Ye, Yushuang Wu, Zizheng Yan, Chenming Zhu, Zhangyang Xiong, Tianyou Liang, Guanying Chen, Shuguang Cui, and Xiaoguang Han. Mvimagnet: A large-scale dataset of multi-view images. In *CVPR*, pages 9150–9161, 2023. 2, 3
- [55] Weixia Zhang, Guangtao Zhai, Ying Wei, Xiaokang Yang, and Kede Ma. Blind image quality assessment via vision-language correspondence: A multitask learning perspective. In *IEEE Conference on Computer Vision and Pattern Recognition*, pages 14071–14081, 2023. 5
- [56] Junsheng Zhou, Jinsheng Wang, Baorui Ma, Yu-Shen Liu, Tiejun Huang, and Xinlong Wang. Uni3d: Exploring unified 3d representation at scale. In *International Conference on Learning Representations (ICLR)*, 2024. 5
- [57] Xingyi Zhou, Vladlen Koltun, and Philipp Krähenbühl. Simple multi-dataset detection. In *Proceedings of the IEEE/CVF conference on computer vision and pattern recognition*, pages 7571–7580, 2022. 3

In this supplementary materials, we provide visual examples and construction details of datasets in Sec. A, implementation details and visual examples of metrics in Sec. B, Prompt construction details in Sec. C, details of the user study in Sec. D, visual comparison of GT23D baselines and additional quantitative comparisons in Sec. E

Appendix A. 3D Datasets Details

A.1. Multi Modal Annotations

More Visual Examples. In our paper, we presented several numerical statistics from the dataset, such as the distribution of aesthetic scores and clip scores. Here, we provide additional visual results. As illustrated in the Fig. 10, the aesthetic scores indeed reflect, to a certain extent, the quality and sophistication of the models. As the aesthetic scores increase, the data displays more elaborate textures and vibrant color distributions. While as illustrated in the Fig. 11, our 3D text data pairs consistently achieved high clip scores.

Coarse-to-Fine Hierarchical Caption. We utilize LLaVA [23] to annotate the dataset captions. As shown in the Fig. 13, Objaverse [6] contains numerous annotation errors, such as emojis or descriptions of model styles, rather than actual descriptions of 3D objects. Cap3D [30] provides relatively rough descriptions lacking detail, while 3DTopia [14] offers more detailed descriptions but includes many meaningless subjective annotations. In contrast, as illustrated, our dataset presents a comprehensive captioning approach that progresses from coarse to fine levels of detail compared to existing annotated datasets. For example, the annotation for a fish includes the keyword "fish" and its associated category, an overall semantic description such as "A cartoon-style rocket ship," and detailed descriptions covering the fish's components and their characteristic attributes. Lastly, we extract localized descriptions from the detailed annotation, such as "Fish body: blue ...," to facilitate more fine-grained evaluations.

To annotate the objects, we used LLaVA by providing it with the front view, side view, and top view of each object, along with a corresponding prompt. LLaVA then generated captions for the objects, as illustrated in Fig. 13. The prompt included specific requirements for generating captions as well as examples.

To make the caption structure cleaner and more comprehensible, and to facilitate the subsequent extraction of components and their attributes, we designed the prompt to require captions to consist of three parts: (1) an overall semantic description of the object, (2) a list of the object's components and their relationships, and (3) detailed descriptions of the components' specific attributes. This approach ultimately resulted in captions with a clear and structured format.

To further validate the impact of accurate and de-

tailed caption annotations on the training effectiveness of the GT23D method, we conduct preliminary training using SeMv-3D [2] under identical settings across different datasets. As illustrated in Fig. 7, it is evident that as the dataset annotations become more precise, the performance of generated outcomes also improves correspondingly.

After generating the captions for objects using LLaVA, we refined the captions further. First, we used LLAMA to simplify the captions by removing redundant descriptions as much as possible. For instance, as shown in Fig. 14, sentences like "... helmet with a gold visor ... The helmet has a gold visor ..." were streamlined by prompting LLAMA to eliminate repetitive content while maintaining the overall structure of the sentences. This resulted in more concise and clear captions.

Subsequently, based on the refined captions, we extracted the semantic subject, components, and their attributes. Using LLAMA again, we provided specific requirements and examples in the prompt, instructing it to output results in a fixed format. LLAMA was tasked with summarizing the semantic subject described in the caption along with its key characteristics. When extracting components, we explicitly required LLAMA to avoid treating attributes such as color, shape, and texture as actual components.

This process ultimately produced a comprehensive description of the object as a whole, along with fine-grained descriptions of its individual components.

A.2. Label-based Organize

In the process of object classification, we first referred to ImageNet [7] and WordNet [47] to define 7 primary categories and 20 secondary categories, which were provided to LLAMA [45] in JSON format. LLAMA was tasked with summarizing the semantic subject described in the captions and attempting to classify the subject into the existing secondary categories wherever possible. If the existing secondary categories were insufficient to encompass the subject, the language model was permitted to introduce new secondary categories. Finally, LLAMA was instructed to output the object's label, primary category, and secondary category in a fixed format.

To ensure LLAMA better understood the task, we provided three examples. We allowed the language model to add only secondary categories while keeping the primary categories unchanged. Through the expansion and merging of secondary categories, we ultimately obtained 28 secondary categories.

A.3. Quality-based Filter

The data filtering process involved multiple stages, as illustrated in the figure. First, we filtered out low-quality objects from the Objaverse dataset based on annotation infor-

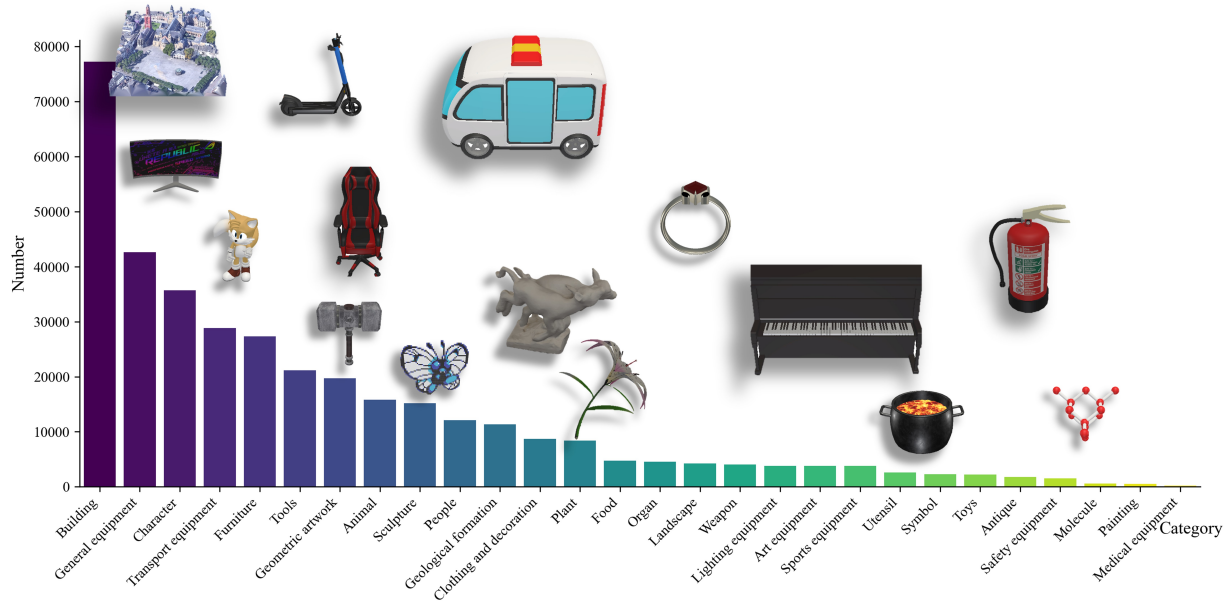


Figure 6. Subcategory distribution visualization and visual examples of our 3D dataset.

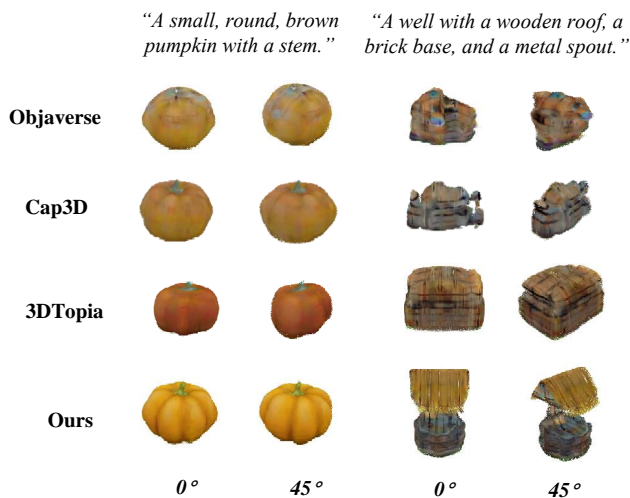


Figure 7. Visual Comparison of SeMv-3D Finetuned in Different Dataset.

mation, such as tags and other attribute fields. For example, objects with the "3dscannerapp" tag, indicating they were created using mobile scanning, were generally of lower quality and thus removed. Next, we applied a connected-component algorithm to compute the fragmentation level of 3D model render images, excluding objects with a fragmentation ratio greater than 1%.

Following this, we calculated the centroid across multiple rendered images from different angles. As shown in

Fig. 9, objects whose centroids were not within the central region were filtered out. We then removed most objects lacking textures, primarily determined by whether the rendered images appeared gray.

After annotating the objects with LLaVA, we excluded captions with vague semantic descriptions. For instance, as shown, the description of a butter loaf as merely "A rectangular object ..." was deemed insufficient for effective model training and evaluation. Additionally, we computed the matching degree between the rendered images and captions, discarding objects with a matching score below a predefined threshold.

Finally, we calculated the aesthetic scores of the objects and removed 3D models with scores below a certain threshold, retaining only visually appealing objects. After these filtering steps, we obtained a high-quality dataset of 3D objects.

The final data distribution of our dataset is shown in Fig. 6, presenting all 28 categories and their corresponding quantities. These range from the most commonly encountered categories in real life, such as Building, to less frequently seen ones like Antique and Safety equipment. Overall, the distribution follows a long-tail pattern.

When calculating aesthetic scores, we divided the dataset into different segments, as shown in Fig. 10. Objects in different segments varied in aesthetic quality, with higher scores generally corresponding to more visually appealing objects. We removed objects with aesthetic scores below 3.6, as those scoring below this threshold were generally

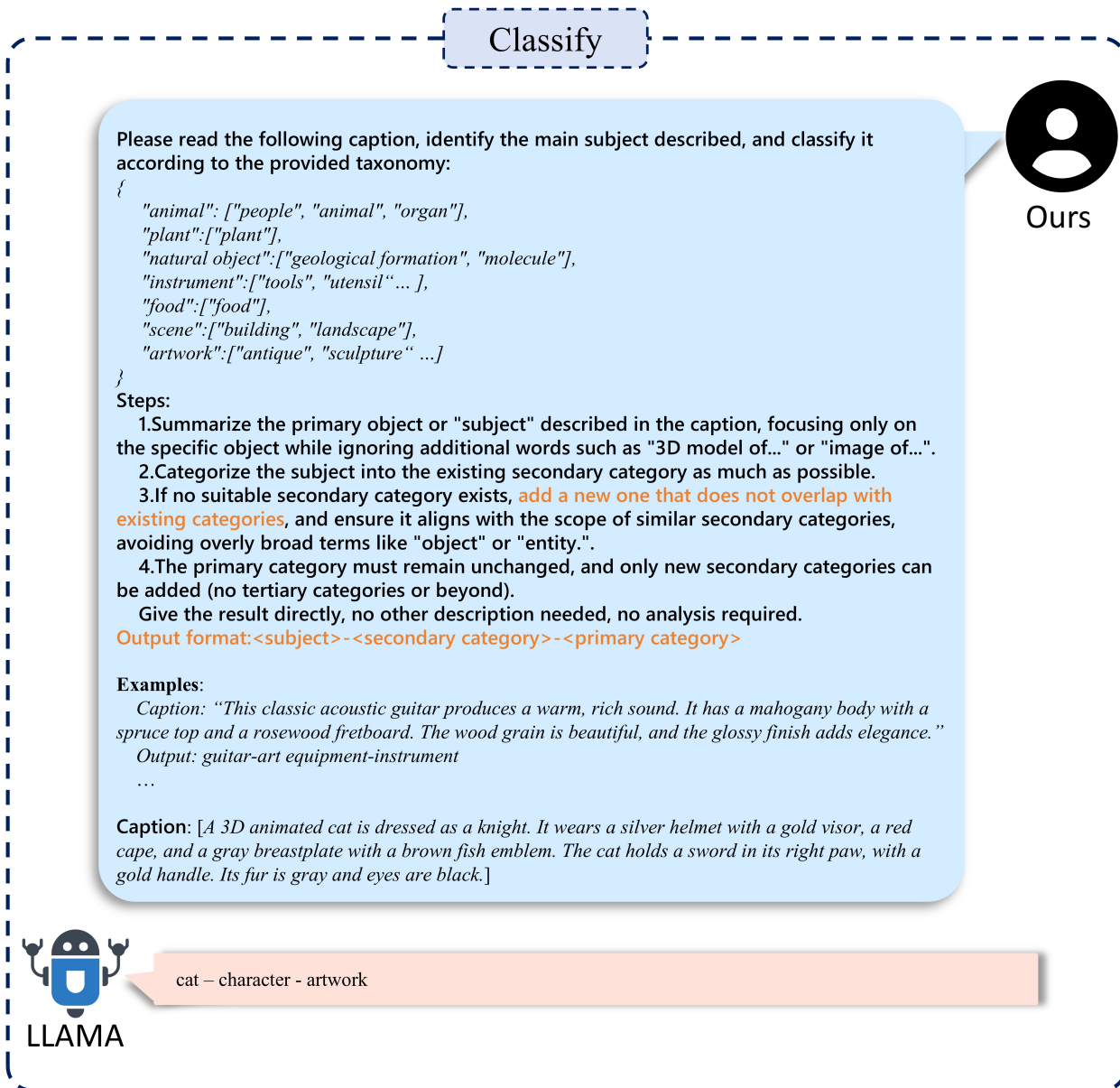


Figure 8. **Illustration of the dataset classification.** Classify caption with the aid of LLaMA.

characterized by monotonous or unbalanced shapes and textures.

To obtain captions that closely match the objects, we calculated the CLIP score based on the rendered images and their captions, as shown in Fig. 11. Lower scores (e.g., below 27) indicated a greater disparity between the caption and the object, often due to issues in describing certain components or attributes. Higher scores (e.g., above 39) demonstrated consistency between the caption and the ren-

dered images, with no descriptive deviations. Ultimately, we removed objects with a CLIP score below 23, as their captions showed significant discrepancies from the objects.

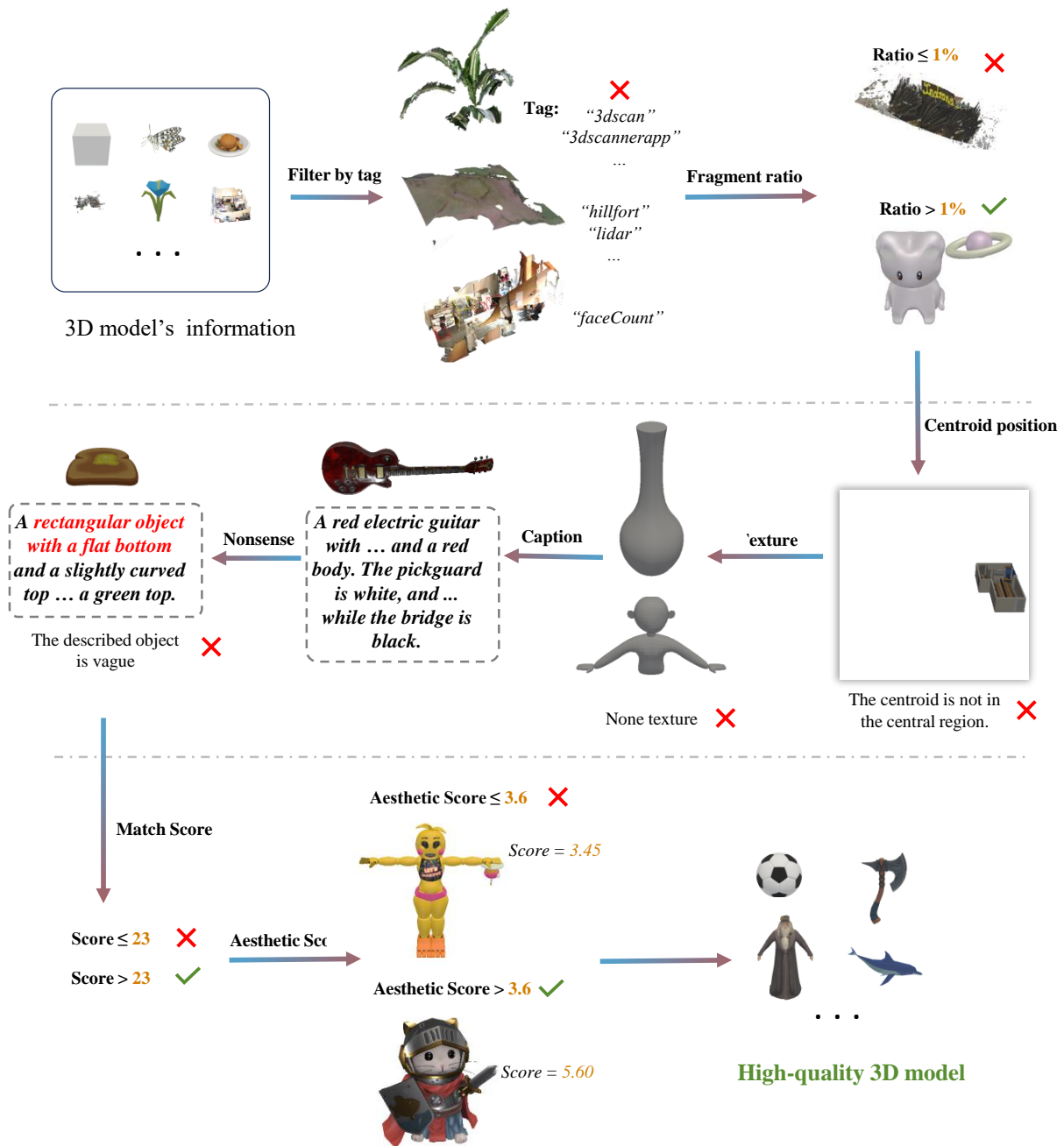
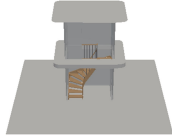
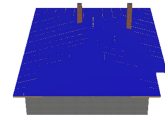
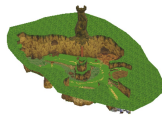


Figure 9. Illustration of Quality-based Filter process details.

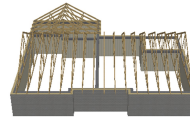
3.6 – 4.1



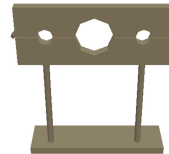
4.1 – 4.6



4.6 – 5.1



5.1 – 5.6



>5.6



Figure 10. Examples of Different Levels of Aesthetic Scores.

23 – 27



A **metal** box with ... a silver lock ... The box has a black handle and a black and silver color scheme.



A blue and gray statue of a knight ... a **helmet**, a sword, and a **shield** on the chest ... **chainmail** is silver.

27 – 31



A red tent ... The tent has a flat floor, a **green** base, ... while the columns and floor are a lighter red.

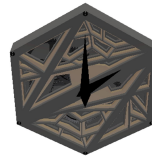


A cartoon ... a small **black nose**, ... character wears a white belt with a gold buckle.

31 – 35



A small brown figurine of a **pig** ... The pig's body and ears are brown, while the base is white.



A hexagonal clock with a black face ... is surrounded by a black border with white geometric patterns.



A 3D model of a room ... the desk is **gray**... and a glass pane with a view of a garden.

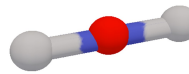


A beige hat with a red and green band. The band has a gold emblem on the front.

35 – 39



A 3D model of a Pokéball. ...has a glossy red and black texture ... and a **black** button.



A molecule model ...are smooth and shiny, and the rod is straight and cylindrical.



A 3D rendering of a candle is shown ... The candle is placed on a white background.

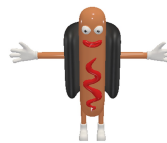


A black bottle of wine is standing upright ... The bottle is black and the base is brown.

>39



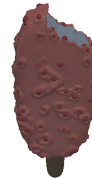
A 3D model of a humanoid figure ... blue pants, and brown shoes ... pom-pom on top.



A 3D animated hot dog character ... dog is standing upright with its arms outstretched.



A 3D model of a superhero in a black suit ... has a belt around the waist. The cape is brown.



A black bottle of wine is standing upright ... The bottle is black and the base is brown.

Figure 11. Examples of Different Levels of Clip Scores.

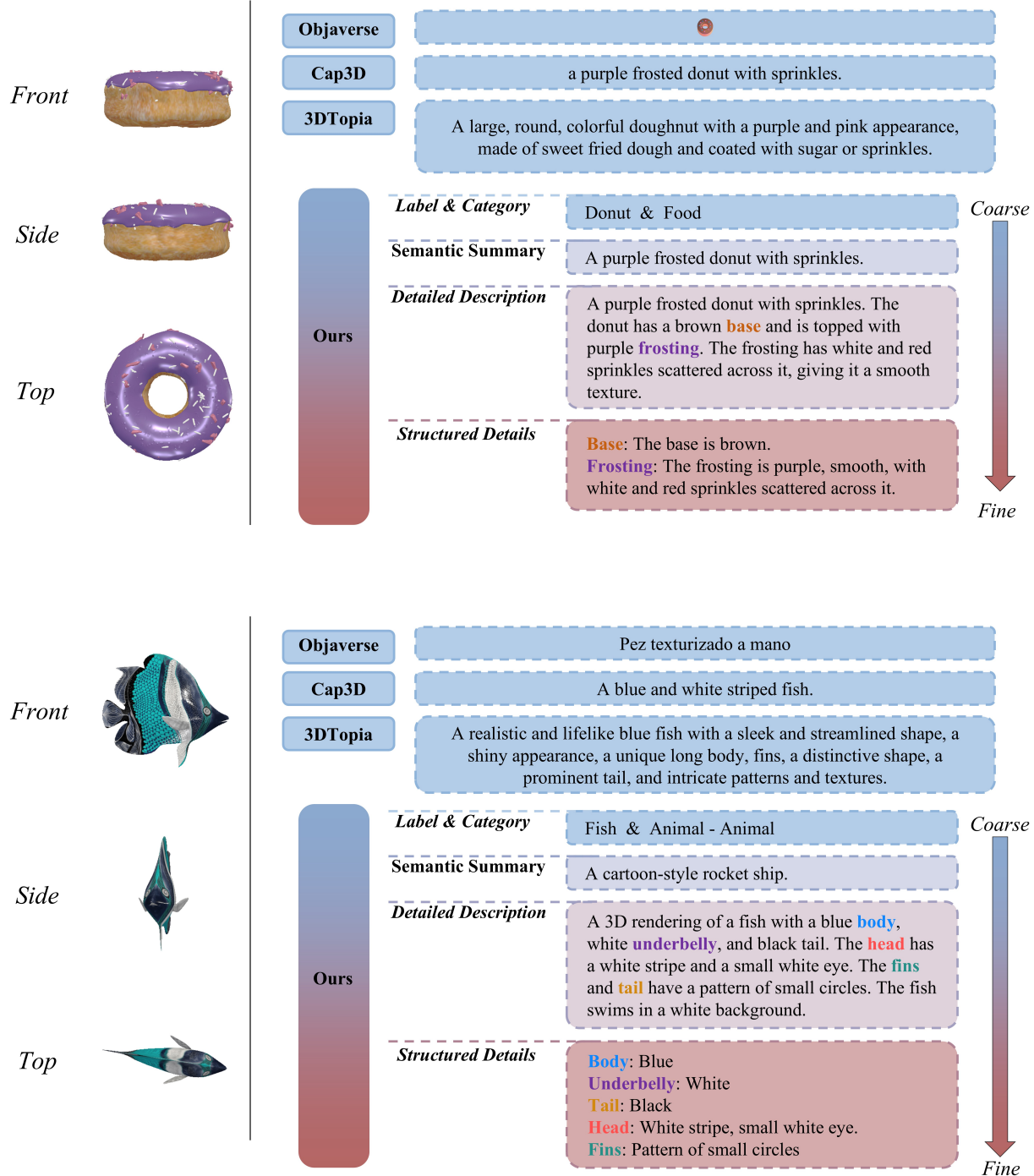


Figure 12. **Comparison of Captions Across Different Datasets.** Compared to other existing datasets, our GT23D-Bench offers more comprehensive captions ranging from coarse to fine-grained levels.

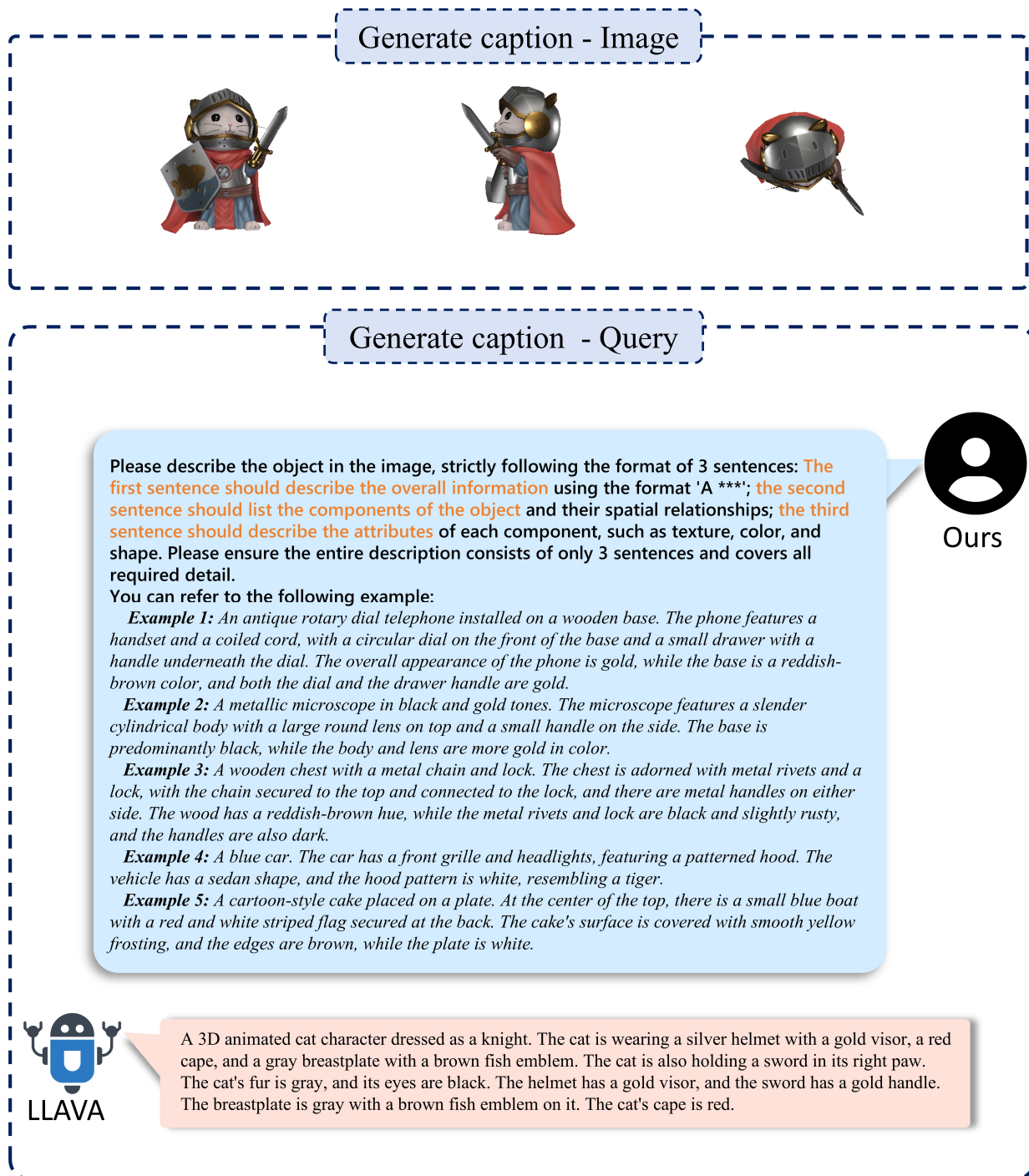


Figure 13. Illustration of caption process for detailed description generation using LLaVA.

Refine caption

Please simplify the following image caption by removing any subjective feelings that do not aid in describing specific objects and eliminating any redundant or repetitive descriptions. Maintain the original structure as much as possible and ensure that the meaning of each part of the caption remains unchanged. Ensure the final caption remains clear and objective. Give the result directly, no other description needed.



Ours

Caption:*[A 3D animated cat character dressed as a knight. The cat is wearing a silver helmet with a gold visor, a red cape, and a gray breastplate with a brown fish emblem. The cat is also holding a sword in its right paw. The cat's fur is gray, and its eyes are black. The helmet has a gold visor, and the sword has a gold handle. The breastplate is gray with a brown fish emblem on it. The cat's cape is red.]*



LLAMA

A 3D animated cat is dressed as a knight. It wears a silver helmet with a gold visor, a red cape, and a gray breastplate with a brown fish emblem. The cat holds a sword in its right paw, with a gold handle. Its fur is gray and eyes are black.

Analyze the following caption and extract the main subject, its components, and their attributes. Provide the results directly without the need for additional description. Please follow these steps:

Subject: Identify the main subject from the caption and provide a brief description of its characteristics.

Components: List the main components of the subject along with corresponding attribute descriptions. Note that components are specific physical entities, while color, shape, texture, and so on are attributes of the components, not the components themselves.

Output Format:

Subject: [Subject description]

Components:

[Component 1]: [Attribute description]

[Component 2]: [Attribute description]

...

example 1:

A 3D model of a bed with a rectangular frame and a flat top. The bed has a sloping headboard and is made of a single piece of gray material. The headboard is elevated compared to the rest of the bed. The bed's surface is smooth, while the headboard has a textured surface.

output:

Subject: A gray bed with a rectangular frame and a flat top.

Components:

The bed's surface: The bed's surface is smooth

Headboard: the headboard is elevated compared to the rest of the bed, with texture.

...

Caption:*[A 3D animated cat is dressed as a knight. It wears a silver helmet with a gold visor, a red cape, and a gray breastplate with a brown fish emblem. The cat holds a sword in its right paw, with a gold handle. Its fur is gray and eyes are black.]*



Ours



LLAMA

Subject: A 3D animated cat dressed as a knight.

Components:

Helmet: silver with a gold visor

Cape: red

Breastplate: gray with a brown fish emblem

Sword: gold handle

Fur: gray

Eyes: black

Figure 14. Illustration of caption refinement for concise description and components extraction using LLAMA.

Appendix B. 3D-Aware Evaluation Metric Details

B.1. Textual-3D Alignment

B.1.1 Textual-Point Cloud Alignment (T-PC)

As shown in Fig. 15, we demonstrate two visual examples evaluated by T-PC. The example of SeMv-3D shows a relatively fragmented shape, leading to a low-quality point cloud. While the example of Shap-E [18] shows a more precise contour and better alignment with text “toy panda”. And our proposed metric of the two examples reflects the visual difference and gives a higher score to the Shap-E that shows better textual-point cloud alignment.

B.1.2 Textual-Multiview Alignment (T-MV)

Three visual examples from VolumeDiffusion [44], Shap-E and MvDream [42] are shown in Fig. 17 evaluated by T-MV. Since VolumeDiffusion demonstrates unrecognizable visual results, its T-MV score (0.25/1) is low. As visual results of MvDream show better correspondence between images and prompts in detail than those of Shap-E, its T-MV score (0.73/1) is higher than T-MV score (0.0.32/1) of Shap-E.

B.1.3 Textual-3D Attribute Alignment(T-Attr)

As shown in a) of Fig. 18, we illustrate the algorithm pipeline of T-Attr. Components prompts of an object (“wooden stand” of an “old telephone with wooden stand ...”) are fed into GroundedSAM [39] to detect corresponding components from rendered multiview images. The detection scores (detection confidence multiplies detection probability) are averaged across components and serve as scores of T-Attr.

And in b) of Fig. 18, visual examples measured by T-Attr are shown. As seen, the mushroom example of Shap-E on the left-up corner owns a ‘brighter’ cap than the example of SeMv-3D on the left-bottom corner, the detection score of which is relatively higher. This further verifies that our T-Attr reflects textual-3D alignment at a fine-grained level.

B.2. 3D Visual Quality

B.2.1 Texture Fidelity

Multi-view Image Quality (MV-IQ). As demonstrated in Fig. 16, examples of Point-E [32], Shap-E and MvDream measured by T-MV are illustrated. It is evident that as the details of multi-view images become increasingly clear, better reflecting the “marble statue” described in the text, the scores provided by MV-IQ consistently increase.

Contour Clarity (CC). To determine whether an image possesses sufficient clarity, we can compare the level of blurriness between the original image I and its blurred version I_{blur} . A greater decrease in sharpness S indicates that the original image is more distinct.

In this section, we provide visual examples and algorithm illustrations of our proposed metrics as follows.

A black and white toy panda bear wearing a black shirt.

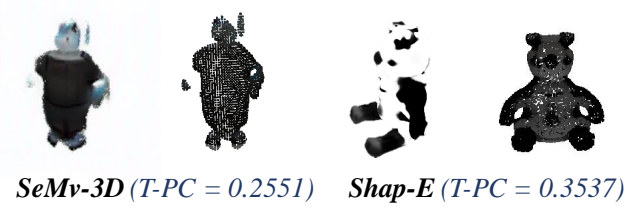


Figure 15. Visual examples of Textual-Point Cloud Alignment.

A marble statue of smooth white stone ... is human,

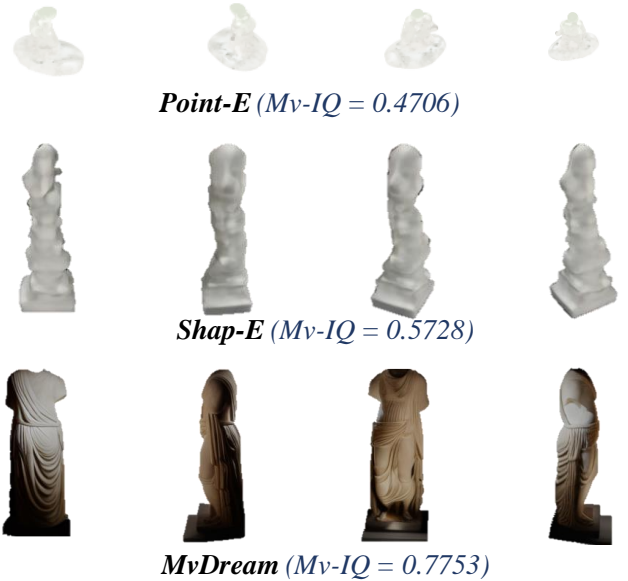


Figure 16. Visual examples of Multi-View Image Quality.

As shown in the left of Fig. 19, to quantify the sharpness, we measure the gradient variation in pixel intensity across the image. For each pixel (x, y) in the image, we compute the product of absolute intensity differences along the x and y directions, as follows:

$$S = \sum_{x,y} |I[x, y] - I[x + 1, y]| \times |I[x, y] - I[x, y + 1]| \quad (11)$$

The larger the value of S , the sharper and clearer the edges of the image content. By assessing the change in S , we can ultimately measure Contour Clarity as follows:

$$Score_{CC} = \frac{S - S_{ori}}{S} \quad (12)$$

As the right visualization results show, the change of sharpness of Shap-E’s elephant before and after blurring is visibly less significant than that of MvDream. Therefore,

MvDream scores higher in the final evaluation. While for 3Dtopia, it is more blurred and exhibits severe ghosting on the surface of objects. Consequently, it scores very low in Contour Clarity.

Texture Richness (TR). The basic idea of TR is to compare the difference between a texture-rich image and a generated rendered view which share the same high-frequency contours. We create these texture-rich images using Stable Diffusion (SD) [40, 46], as illustrated on the left of Fig. 20. Specifically, we invert the generated rendered view into the noise space using DDIM sampling to strip away low-level details while preserving high-level contours. At a specific timestep t_i during the inversion process, we halt the inversion and denoise the intermediate representation back into pixel space, conditioned on the same prompt as the generated rendered view.

Less detailed images provide Stable Diffusion with more flexibility to generate creative details. Consequently, examples lacking vivid and detailed textures exhibit larger differences from the generated texture-rich images, as shown by the visual results on the right of Fig. 20. In contrast, the example of MvDream is vividly realistic and its created texture-rich image is highly similar to itself.

To prevent excessive detail loss during the inversion process, an appropriate timestep t_i needs to be selected. As shown in Fig. 21, the total timestep is 100. If the t_i is too large (e.g., $t_i = 90$), essential high-frequency information, such as spatial arrangement, is almost lost. If the t_i is too small (e.g., $t_i = 40$), most original details are retained, leaving limited creative space for Stable Diffusion. Consequently, to balance contour preservation with sufficient generative flexibility, we select $t_i = 50$ as the optimal timestep.

B.2.2 Geometry Correctness

3D Alignment (3D-Ali). To validate that generated 3D shapes are geometrically aligned with real-world shapes, we design 3D-Ali to measure the distance between generated shapes and real-world shapes. Specifically, we sample caption-3D data pairs from our well-curated high-quality 3D datasets, and feed the caption into GT23D baselines to generate 3D shapes. Then we unify representations of the generated 3D and ground-truth 3D into point cloud. These two point clouds are fed into the open domain pretrained point cloud feature extractor, the 3D encoder of Uni3D, and obtain corresponding 3D features. Finally, we calculate the cosine similarity between the two 3D features as 3D-Ali.

Such designs avoid voxel-level comparison and emphasize semantical alignment between two 3D shapes conditioned on the same prompt. As shown in Fig. 22, compared to the ground truth, the shape produced by Shap-E more closely aligns with the geometric structure of a skull, whereas the results from 3DTopia exhibit an unreasonable

A long bus with large panoramic windows and sturdy wheels beneath.

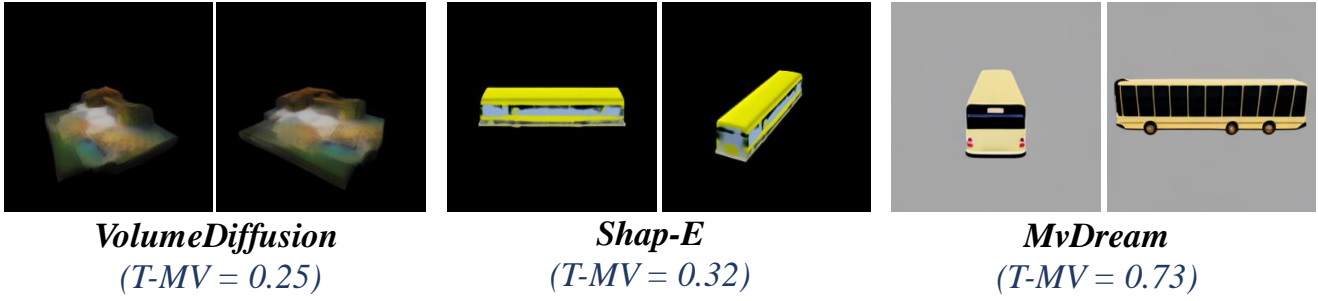


Figure 17. Visual examples of Textual-MultiView Alignment

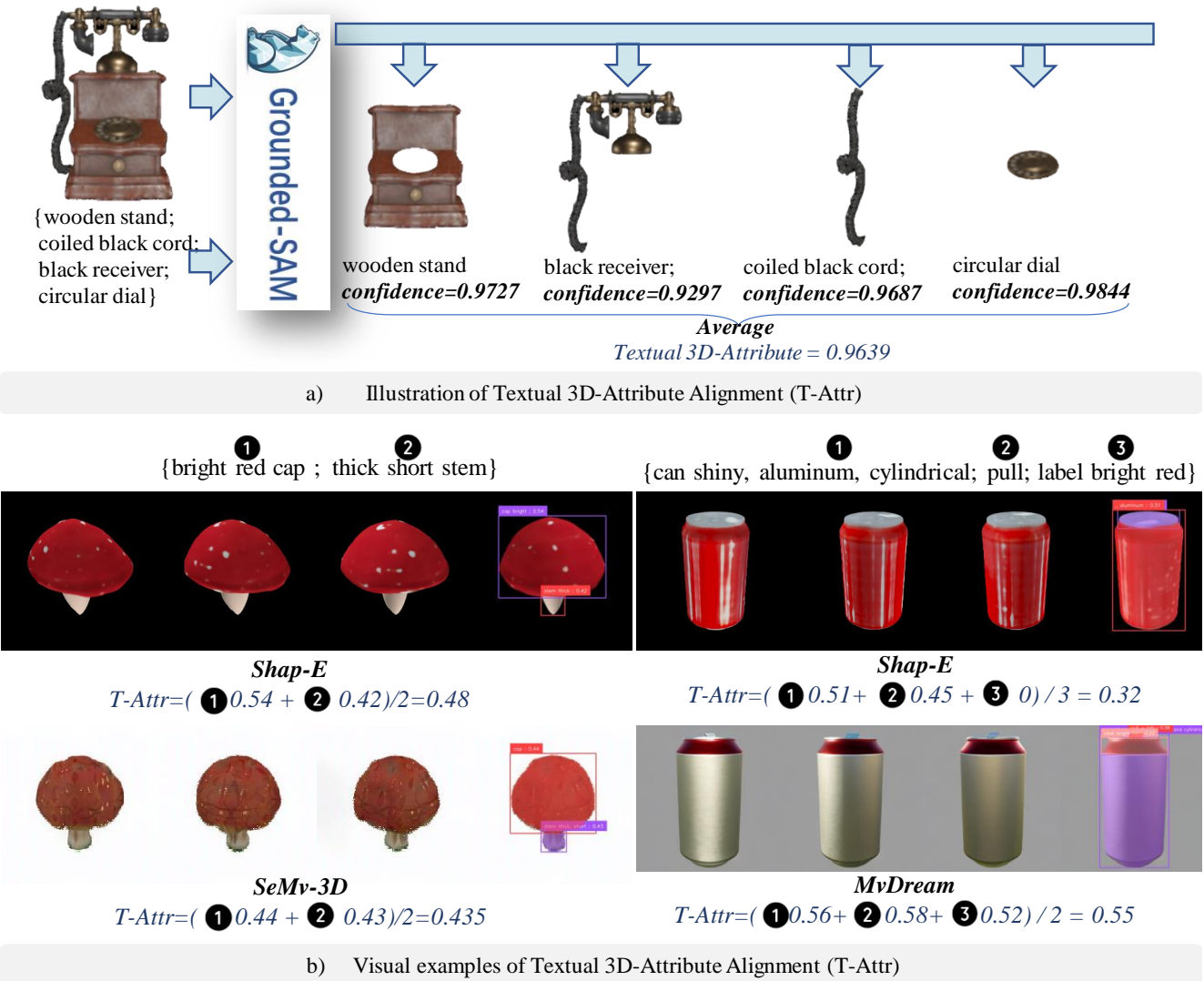


Figure 18. **Textual 3D-Attribute Alignment.** a) Illustration of Textual 3D-Attribute Alignment. b) Visual examples of Textual 3D-Attribute Alignment.

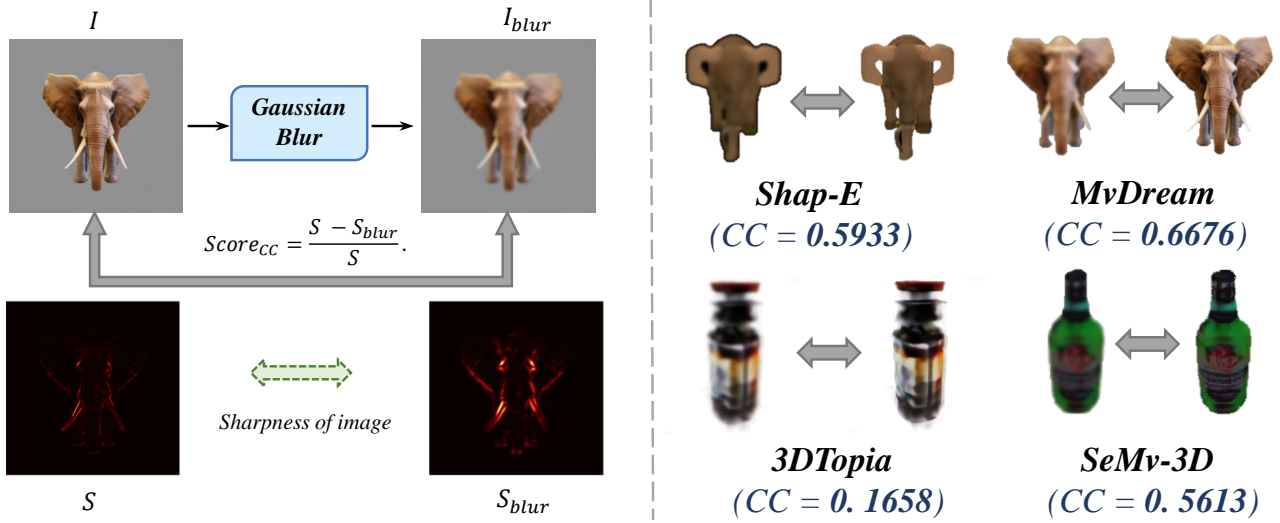


Figure 19. Illustration of Contour Clarity(left) and visual examples of Contour Clarity(right).

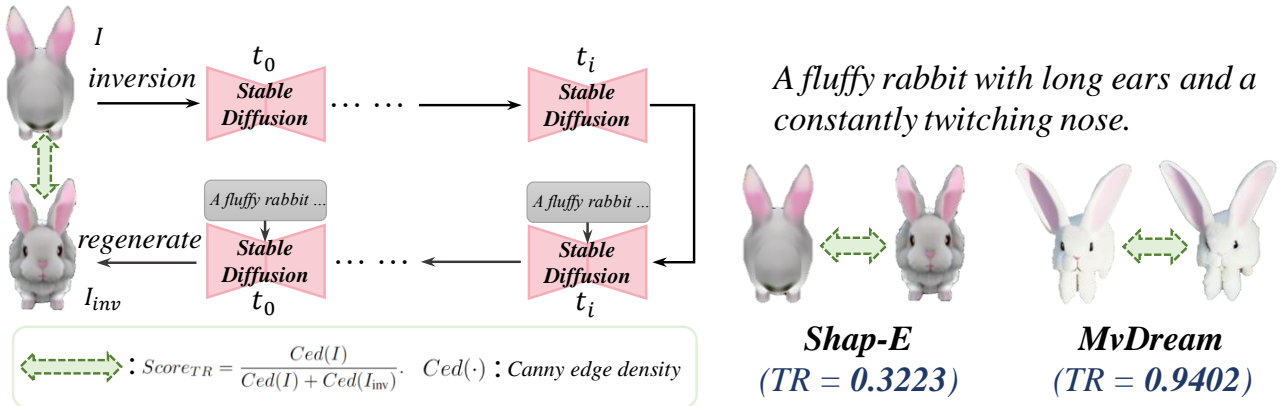


Figure 20. Illustration of Texture Richness(left) and visual examples of Texture Richness(right).

shape and lower quality.

Shape Completeness (Shape-C). As demonstrated in Fig. 23, Shape-C could reflect the extent of fragmented parts in generated images. The examples of 3DTopia own the most outlier noises compared to those of SeMv-3D and Shap-E, and thus obtain the lowest Shape-C score. Since the examples of SeMv-3D show slightly granular object edges compared to those of Shap-E, its Shape-C score is slightly lower than that of Shap-E.

Geometric Validity (Geo-V). As shown in Fig. 24, we visualize the reasoning process of ChatGPT-4o [33] about how they score a generated 3D object in Geometric Validity. The reasoning process contains three main parts: Geometric Reasonableness judges whether the geometric shape is reasonable and obeys real-world physical rules. Geometry Alignment measures whether the geometric shape is recognizable and aligns with the object type in the given prompt.

Geometric Quality considers whether the 3D shape is of high quality without discontinuity or fragmented noises. Each part is evaluated on a full score of 100 points. To assess whether the generated object’s geometry exhibits any issues, we prompt ChatGPT-4o with visual examples for judgment. For instance, as illustrated by the example of the ship, methods such as Shap-E are identified to have flaws, including breakage and structural inconsistencies.

B.2.3 Multi-View Consistency

We have outlined the detailed operational workflow for the Multi-View Consistency metric, as illustrated in the Fig. 25. Using Depth-Anything [53], depth maps are generated for the source view. These depth maps, combined with the corresponding RGB images, are converted into point clouds. Subsequently, sampling other viewpoints allows for verifying the consistency of object generation across multiple tar-

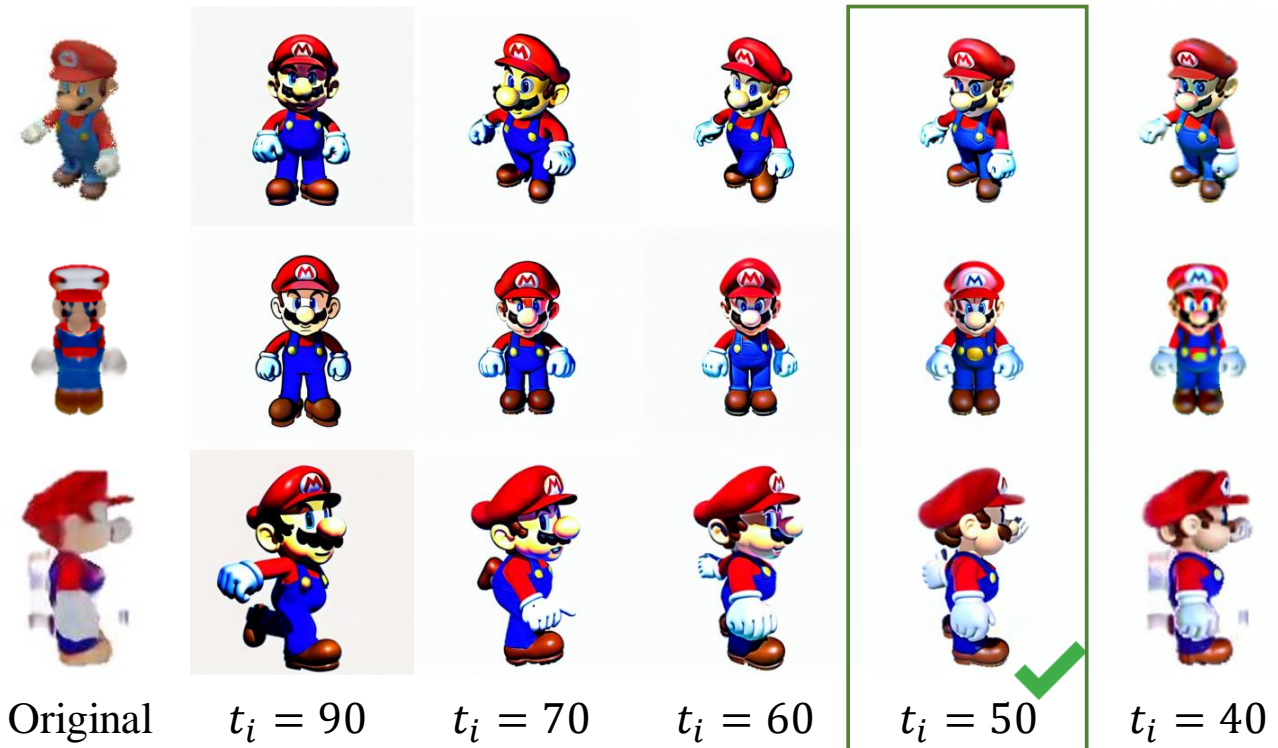


Figure 21. Choice of t_i in inversion process of Stable Diffusion in Texture Richness.

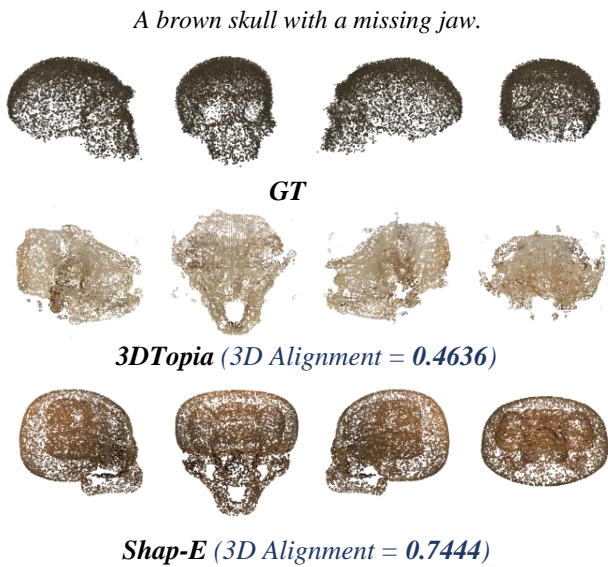


Figure 22. Point cloud examples of 3D Alignment.

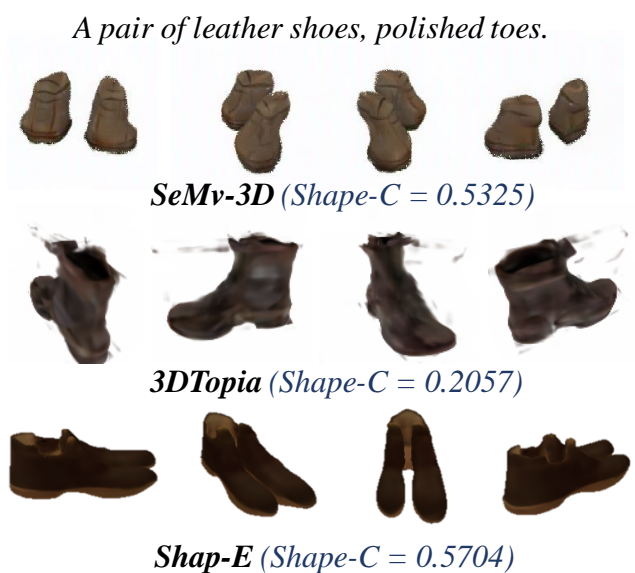


Figure 23. Visual examples of Shape Completeness.

get views. As shown in the bottom section of the figure, the necklace demonstrates a lack of consistency between two viewpoints, resulting in a low score (0.6188/1). In contrast, the purple chair achieves a high score (0.8981/1) due to its

significant consistency across views.

Do

Please score the geometric qualities of 3D objects generated from text descriptions according to the following criteria. Note that each 3D object generated from the text description is a single, background-free object. Each criterion should be scored from 0 to 100, and each 3D object's total score is the sum of the scores for each criterion. If an object does not meet the following evaluation standards, it should receive a low score, while objects that are more perfectly aligned with these standards can receive higher scores. Only a very few objects that perfectly meet all of the requirements in these evaluation criteria should receive full marks. The criteria for evaluating the geometric qualities of the object are as follows:

1. **Geometric Reasonableness**: Ensure that all parts of the object have reasonable proportions and conform to real-world scales. If there are unreasonable or repeated structures or duplicate parts, the object should receive a low score. Check for visual discrepancies from different perspectives, and verify consistency across the three views (front view, side view, and top view).

2. **Geometry Alignment**: In the absence of additional hints, evaluate whether the object's geometric shape intuitively suggests its category. The geometric features of the model should match the characteristics of the object described in the text to facilitate recognition. Objects that are difficult to identify or have low recognizability should receive very low scores.

3. **Geometric Quality**: The object should not have fractures, discontinuities, or illogical dents. Specifically, fractures may appear as cracks or holes on the surface of the object. Fractured edges are often irregular, giving an impression of an incomplete object. Discontinuities refer to

A ship with a streamlined hull, towering masts, and billowing white sails.



Point-E

$$Geo-V = (30+20+20)/300=0.2333$$

Geometric Reasonableness: The proportions and scale are challenging to assess due to the small size and lack of clarity.... **Score1: 30 / 100**

Geometry Alignment: The object's geometric shape is difficult to categorize due to its unclear and small presentation.... **Score2: 20 / 100**

Geometric Quality: The object appears to have some irregularities and lacks detail due to its small scale in the image.... **Score3: 20 / 100**



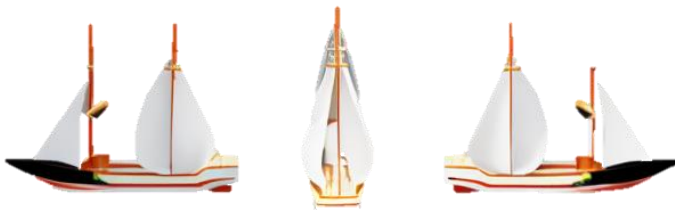
Shape-E

$$Geo-V = (50+45+40)/300=0.45$$

Geometric Reasonableness: ... there are some irregularities when viewed from different angles. Masts and sails appear uneven.... **Score1: 50 / 100**

Geometry Alignment: ...The ship is generally recognizable. However, some details appear vague, affecting clear category.... **Score2: 45 / 100**

Geometric Quality: There are visible discontinuities and possible fractures, particularly around the sails and mast.... **Score3: 40 / 100**



MvDream

$$Geo-V = (85+80+75)/300=0.8$$

Geometric Reasonableness: The 3D object displays generally reasonable proportions and adheres well to real-world scales.... **Score1: 85 / 100**

Geometry Alignment: ...The details of the masts and sails correspond reasonably to the expected characteristics of a sailboat.... **Score2: 80 / 100**

Geometric Quality: object appears free from fractures. However, the level of detail could be improved for further refinement. **Score3: 75 / 100**

Figure 24. Illustration of reasoning process on Geometric Validity using ChatGPT-4o.

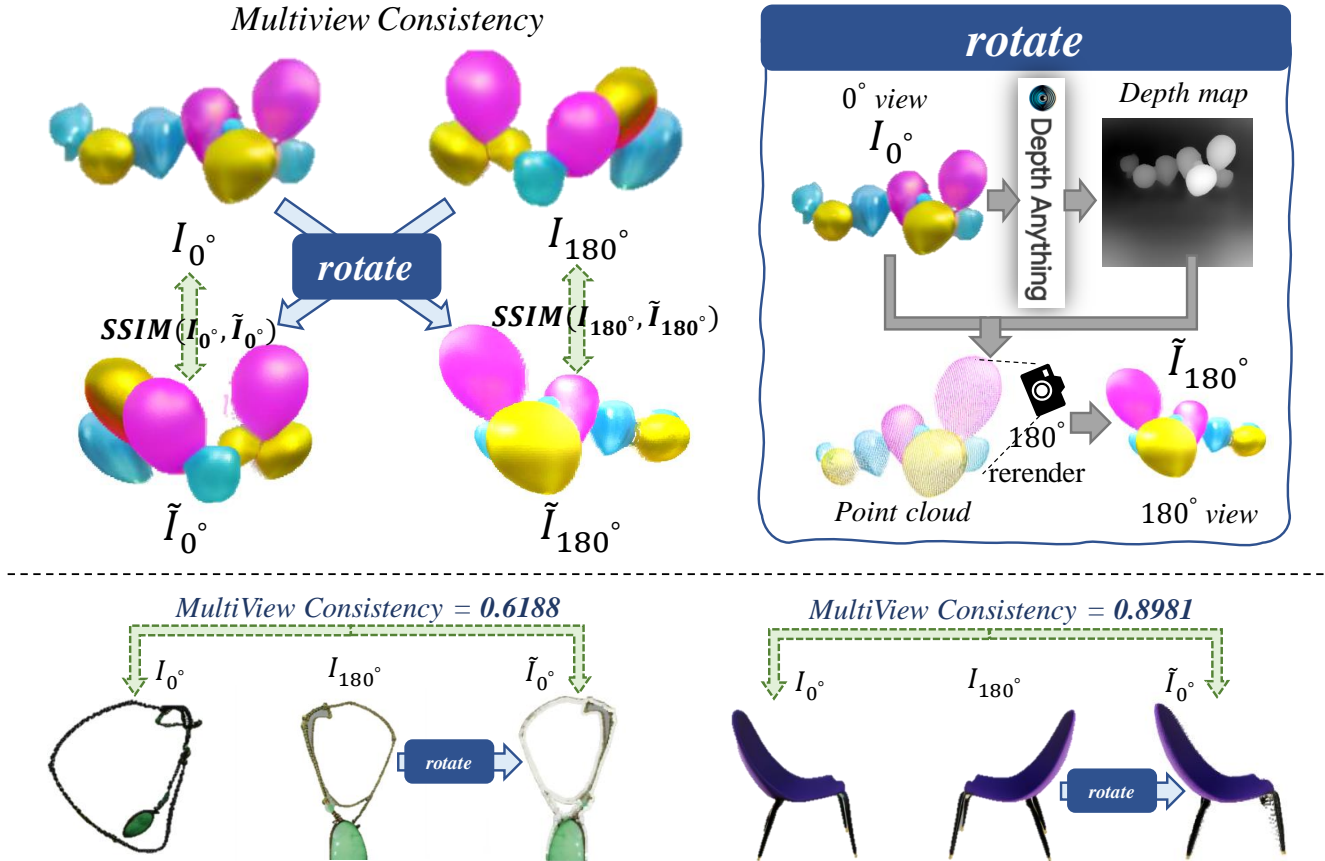


Figure 25. Illustration of Multi-View Consistency(up) and visual examples of Multi-View Consistency(bottom).

Appendix C. Prompt Set Construction

Dataset Samples. From the filtered high-quality dataset, we randomly sample 30 captions of varying granularity (Coarse or Fine) per category to serve as the test prompt set. By employing this sampling strategy, which ensures uniformity across major categories and captures the long-tail distribution within subcategories, we aim to validate the GT23D method’s generation capability under a distribution similar to real-world scenarios.

Open-domain Construction. To better evaluate the generalization capability of text-to-3D generation methods, we utilized ChatGPT-4o to generate 200 prompts. These prompts were designed to vary across three levels of creativity and complexity. Creativity was categorized into three types: common objects, uncommon objects, and imaginary objects that do not exist in reality. Complexity was determined based on the level of detail in the prompt descriptions. In terms of distribution, the quantity of prompts decreases progressively from simple common objects to complex imaginary ones, reflecting the long-tail distribution

commonly observed in real-world (user scenarios). Examples of these prompts are shown in Fig. 26.

Appendix D. User Study Details

Caption User-Study. We conduct a comparative user-study to evaluate the captions dataset (human alignment and training boost) from Objaverse, 3DTopia, Cap3D, and our GT23D-Bench. Fig. 27 is one example from the user-study. To ensure fairness, the order of captions for each question is randomized.

Metrics User-Study. To assess whether the evaluation results of our metrics are reasonable and aligned with human judgments, we also conduct a user-study covering ten dimensions, as illustrated in Fig. 28.

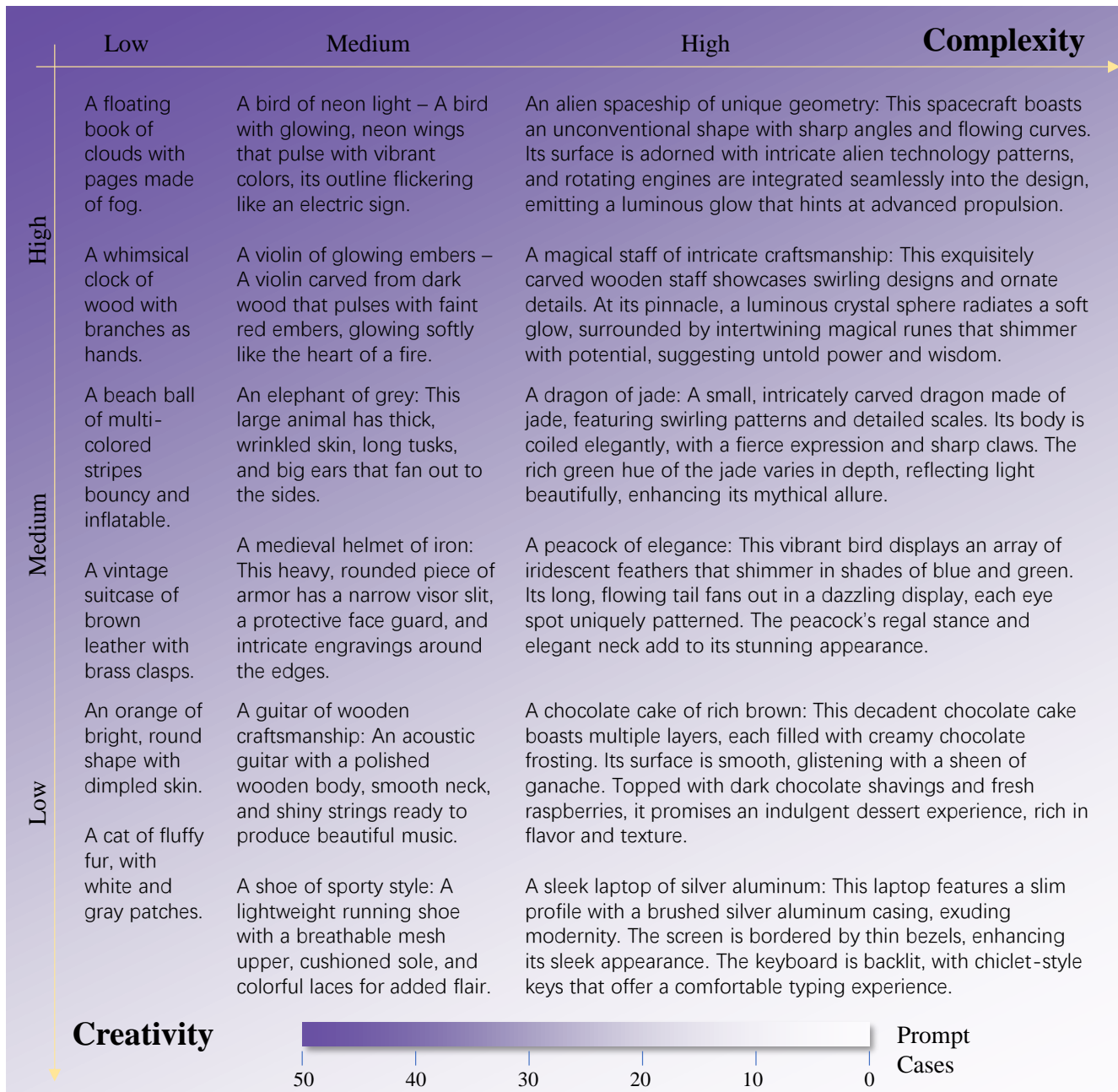


Figure 26. Prompt construction process with different prompt creativity and prompt complexity.

* 01 Please observe the 3D model and review the corresponding four text descriptions. Evaluate them comprehensively based on factors such as accuracy, level of detail, and ease of understanding. Assign appropriate scores (you may give higher scores to descriptions you find better and lower scores to those you find less satisfactory).



Dissatisfied Somewhat satisfied Very Satisfied

3december Choco Cake

0 1 **2** 3 4 5 6 7 8 9 10

A three-tier chocolate cake with donuts and pretzels on top, on a stand.

0 1 **2** 3 4 5 6 7 8 9 10

A large multi-layered chocolate cake with chocolate frosting and chocolate chips, displayed on a white plate.

0 1 2 3 4 5 **6** 7 8 9 10

A two-tiered chocolate cake with a white frosting drizzle. The cake is placed on a gray metal stand with a round base and a cylindrical column. The frosting drizzle is dark brown, and the cake has a smooth texture. The stand has a matte finish.

0 1 2 3 4 5 6 7 **8** 9 10

Figure 27. Questionnaire survey of user study evaluating caption from different datasets.

* 01 Caption:
A dragon with a purple body, green wings, and green head. The dragon has a long body with a tail and wings.

Realistic 3D Point Cloud:



Generated 3D point cloud:



Multi-view image of generated 3D PC:



Please rate the 3D objects generated from text based on the following evaluation criteria.

Totally inconsistent Basically consistent Totally consistent

Textual-Point Cloud Alignment: Does the point cloud layout of the 3D model align with the text description, i.e., are the generated model's outline and overall structure consistent with the description?

0 1 2 3 4 5 6 7 8 9 10

Textual-MultiView Alignment: When viewing the 3D model from different angles, does it still maintain a high degree of consistency with the text description?

0 1 2 3 4 5 6 7 8 9 10

Textual-3D Attribute Alignment: The accuracy of the generated model in reflecting the attributes described in the text (e.g., highlighted in bold and blue attributes such as color, size, and specific features).

0 1 2 3 4 5 6 7 8 9 10

Detail Richness, which measures the complexity and resolution of fine surface details.

0 1 2 3 4 5 6 7 8 9 10

Edge Sharpness, which assesses the clarity and definition of contours and edges.

0 1 2 3 4 5 6 7 8 9 10

Multi-view Image Quality, which captures the aesthetic realism of the texture across different views

0 1 2 3 4 5 6 7 8 9 10

Point cloud similarity, semantic alignment with realistic 3D point cloud representations.

0 1 2 3 4 5 6 7 8 9 10

Shape completeness, verifying that models maintain a whole, unfragmented form; and

0 1 2 3 4 5 6 7 8 9 10

Geometric validity, assessing whether the model's geometry aligns with physical-world constraints.

0 1 2 3 4 5 6 7 8 9 10

* 02 Multi-view Images:



Multi-View Consistency: Whether the model's visual appearance and details remain consistent when viewed from different angles in multi-view images.

Totally inconsistent Basically consistent Totally consistent

0 1 2 3 4 5 6 7 8 9 10

Figure 28. Questionnaire survey of user study evaluating generation quality from different dimensions.

Appendix E. More Experiment Results

In the main paper, we present the multidimensional performance of various GT23D methods across different categories of prompt sets. Here, we supplement these findings with visual comparison results for two additional categories, food and animals, as well as a detailed quantitative comparison across six categories.

Visual Comparisons. In these two categories of Fig. 29, we observe that fine-tune-based methods achieved a significant advantage. It seems that prior-based methods share a common issue in generating details. For instance, the generation of facial features or the layers within a hamburger—textures that are highly detailed—are challenging to generate accurately. This results in overall performance issues, such as weak semantic alignment, incomplete component generation, and insufficiently rich and clear textures.

Quantity Comparisons. From the numerical analysis presented in Tab. 5, we observe that fine-tune-based methods like MVDream achieve excellent performance in image quality. In contrast, prior-based methods demonstrate strengths in 3D consistency. Regarding texture richness, shape integrity, and text alignment, we find that although each method has its strengths and weaknesses, they are overall relatively balanced.

Future Look Up. Looking forward, we can anticipate the following trends in GT23D research: 1. Fine-tune-based methods need to overcome the limitations of multi-view generation, achieving arbitrary view generation and addressing consistency across views. 2. Prior-based methods require alignment with the capabilities of existing mainstream visual generation models in detail generation, leveraging and preserving the visual generation knowledge from pre-trained models. 3. GT23D techniques currently lag in texture richness, edge clarity, and component alignment. To achieve the widespread application of GT23D methods, similar to mainstream general vision generation models like SD [40], these areas need to be significantly improved.

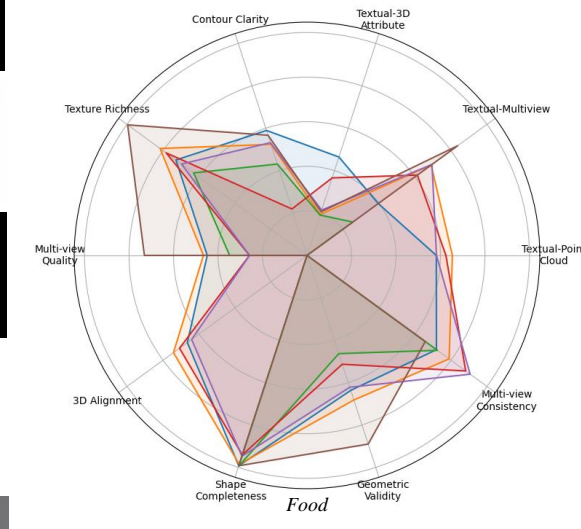
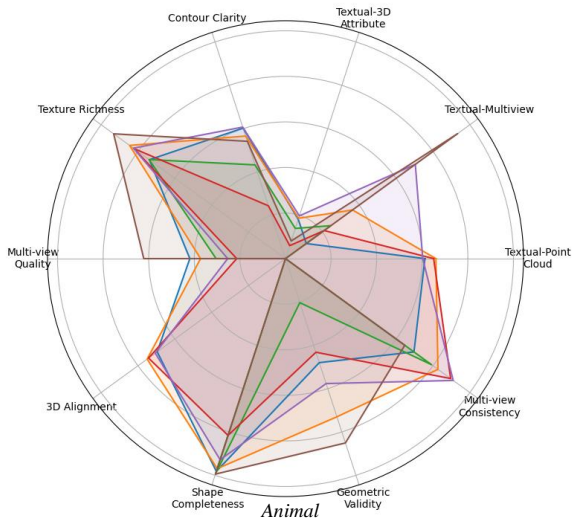
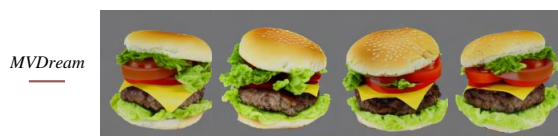
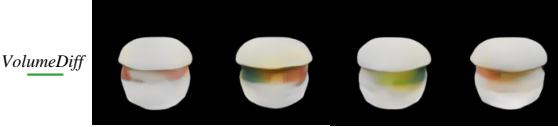
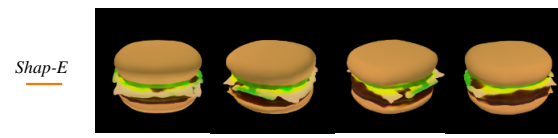


Figure 29. Visual comparison of different GT23D methods in Animal & Food categories.

Category	Method	Textual-PointCloud	Textual-MultiView	Textual-Attribute	Texture Fidelity			Geometry Correctness			Multi-View Consistency
					TR	CC	Mv-IQ	3D-Ali	Shape-C	Geo-V	
Plant	Point-E	0.6109	0.8492	0.5115	0.7875	0.6161	0.4204	0.7391	0.9884	0.5733	0.6963
	Shap-E	0.6526	0.8207	0.1316	0.8684	0.5758	0.3391	0.7600	0.9680	0.7553	0.8688
	VolumeDiffusion	-	0.3115	0.3995	0.7862	0.4416	0.3045	-	0.9932	0.5200	0.7586
	3DTopia	0.6341	0.8335	0.1263	0.8930	0.2339	0.2256	0.7355	0.8636	0.5233	0.8865
	SeMv-3D	0.6026	0.2925	0.1422	0.8878	0.5708	0.2630	0.6831	0.9455	0.7100	0.9191
	MVDream	-	0.8810	0.6102	0.9955	0.6597	0.7424	-	0.9936	0.8420	0.5811
Instrument	Point-E	0.6104	0.5990	0.4047	0.7845	0.6123	0.5012	0.6854	0.9599	0.5300	0.7227
	Shap-E	0.6526	0.8349	0.2089	0.8709	0.5452	0.4627	0.7119	0.9894	0.6567	0.8222
	VolumeDiffusion	-	0.3294	0.3180	0.7182	0.4425	0.3213	-	0.9943	0.3700	0.7863
	3DTopia	0.6200	0.4029	0.2308	0.8459	0.2303	0.2539	0.6839	0.9164	0.5967	0.8816
	SeMv-3D	0.5678	0.4736	0.2397	0.8013	0.6019	0.2825	0.6321	0.9294	0.7433	0.8989
	MVDream	-	0.5735	0.4000	0.9654	0.5522	0.7655	-	0.9912	0.8733	0.6511
Scene	Point-E	0.5783	0.2152	0.1473	0.7818	0.6237	0.4838	0.6366	0.9371	0.2900	0.7548
	Shap-E	0.6269	0.5724	0.4186	0.8269	0.5601	0.3997	0.6959	0.9896	0.3500	0.8235
	VolumeDiffusion	-	0.1619	0.1370	0.7515	0.4301	0.2789	-	0.9943	0.1633	0.7597
	3DTopia	0.6052	0.3935	0.3060	0.8031	0.2412	0.2546	0.6559	0.9629	0.5467	0.8798
	SeMv-3D	0.5664	0.3703	0.2361	0.7913	0.5736	0.2815	0.6150	0.9690	0.5267	0.8890
	MVDream	-	0.9547	0.4460	0.9943	0.6139	0.7095	-	0.9911	0.8440	0.6189
Food	Point-E	0.5814	0.3960	0.4642	0.7284	0.5895	0.4483	0.6650	0.9928	0.6367	0.7194
	Shap-E	0.6538	0.6898	0.1937	0.8163	0.5240	0.4655	0.7420	0.9857	0.6820	0.7897
	VolumeDiffusion	-	0.2549	0.1902	0.6300	0.4310	0.3477	-	0.9946	0.4633	0.7245
	3DTopia	0.6246	0.6134	0.3658	0.7829	0.2191	0.2585	0.7084	0.9411	0.5133	0.8820
	SeMv-3D	0.5822	0.6945	0.2139	0.6974	0.5321	0.2580	0.6410	0.9473	0.6220	0.9067
	MVDream	-	0.8371	0.2060	0.9967	0.5669	0.7309	-	0.9923	0.8900	0.6573
Artwork	Point-E	0.1585	0.2981	0.2196	0.7060	0.5920	0.4061	0.6468	0.9949	0.4167	0.6776
	Shap-E	0.6562	0.6826	0.2290	0.7525	0.5500	0.4195	0.7285	0.9641	0.5600	0.7406
	VolumeDiffusion	-	0.3577	0.1028	0.7027	0.4546	0.2935	-	0.9934	0.2667	0.7689
	3DTopia	0.6310	0.8121	0.1910	0.7968	0.2491	0.2096	0.7049	0.8710	0.5067	0.8891
	SeMv-3D	0.5933	0.6583	0.1246	0.8001	0.5914	0.2506	0.6446	0.9396	0.5800	0.8901
	MVDream	-	0.9164	0.1888	0.9325	0.5406	0.6386	-	0.9945	0.8387	0.6144
Animal	Point-E	0.6118	0.1127	0.1814	0.7383	0.6023	0.4197	0.6957	0.9818	0.4800	0.6967
	Shap-E	0.6598	0.3635	0.1861	0.8452	0.5658	0.3725	0.7503	0.9692	0.7300	0.8267
	VolumeDiffusion	-	0.2462	0.1395	0.7397	0.4326	0.3045	-	0.9943	0.2033	0.7920
	3DTopia	0.6500	0.2098	0.0600	0.8218	0.2440	0.2139	0.7425	0.8159	0.4320	0.8956
	SeMv-3D	0.6021	0.7040	0.1974	0.8250	0.6071	0.2535	0.7061	0.9281	0.5767	0.9095
	MVDream	-	0.9338	0.0814	0.9319	0.5415	0.6218	-	0.9944	0.8507	0.6469

Table 5. Quantitative comparison of different GT23D baselines using metrics of GT23D-Bench in 6 different categories. The higher scores indicate better performance. Since VolumeDiffusion and MVDream do not output explicit 3D representations, their scores are absent in Textual-PointCloud and 3D-Ali which need point clouds.